

A time-varying network model for sexually transmitted infections accounting for behavior and control actions

Original

A time-varying network model for sexually transmitted infections accounting for behavior and control actions / Frieswijk, K.; Zino, L.; Cao, M.. - In: INTERNATIONAL JOURNAL OF ROBUST AND NONLINEAR CONTROL. - ISSN 1049-8923. - ELETTRONICO. - 33:9(2023), pp. 4784-4807. [10.1002/rnc.5930]

Availability:

This version is available at: 11583/2977924 since: 2023-05-10T14:02:14Z

Publisher:

John Wiley and Sons Ltd

Published

DOI:10.1002/rnc.5930

Terms of use:

This article is made available under terms and conditions as specified in the corresponding bibliographic description in the repository

Publisher copyright

(Article begins on next page)

A time-varying network model for sexually transmitted infections accounting for behavior and control actions

Kathinka Frieswijk¹ | Lorenzo Zino² | Ming Cao³

Faculty of Science and Engineering,
University of Groningen, Groningen, The
Netherlands

Correspondence

Kathinka Frieswijk, Faculty of Science
and Engineering, University of
Groningen, Nijenborgh 4, 9747 AG
Groningen, The Netherlands.
Email: k.frieswijk@rug.nl

Funding information

H2020 European Research Council,
Grant/Award Number:
ERC-CoG-771687

Abstract

In this article, we propose a stochastic network model for the spread of common sexually transmitted infections (STIs). The model expands the standard susceptible–infected–susceptible model by incorporating asymptomatic infected individuals—who are unaware that they are posing a health threat to themselves and the population—and individuals' behavioral preferences with regard to the use of protective measures during encounters. Behavioral preferences evolve according to a nontrivial mechanism accounting for the cost of using protection, the perceived risk, and persuasive effects due to sexual encounters with different-minded individuals. The disease spreads on a time-varying network of sexual contacts, generated using a mechanism inspired by continuous-time activity-driven networks. Such a network accounts for regular partners and casual encounters, which are regulated by a negotiation process that accounts for the individuals' behavioral preferences. Finally, three control measures are included in the model: (i) condom (social) marketing campaigns, (ii) routine screening at STI clinics, and (iii) partner notification. We use a mean-field approach to analytically derive the epidemic threshold in the limit of large-scale populations, in the absence of a partner network, for two distinct negotiation processes. Our results indicate that routine screening is key to the eradication of local outbreaks, while condom marketing campaigns become effective only when combined with screening. Monte Carlo simulations are then employed to extend our analytical findings, casting lights on the role of the partner network and on partner notification as a control measure in the spread of STIs.

KEYWORDS

activity-driven network, epidemics models, nonlinear models and systems, sexually transmitted infections, stability

1 | INTRODUCTION

Sexually transmitted infections (STIs) such as syphilis, chlamydia, trichomoniasis, and gonorrhea have been present and widely diffused in the population for many a century, some believe ever since the origin of mankind.¹ A recent study from

This is an open access article under the terms of the [Creative Commons Attribution](https://creativecommons.org/licenses/by/4.0/) License, which permits use, distribution and reproduction in any medium, provided the original work is properly cited.

© 2021 The Authors. *International Journal of Robust and Nonlinear Control* published by John Wiley & Sons Ltd.

the United States (US) Centers for Disease Control and Prevention estimated that more than 20% of the US population is currently affected by an STI.² If left untreated, STIs can lead to serious health problems among which, but not exclusively, stillbirths, infertility, chronic neurological problems, and cancer.³ Since the discovery of penicillin by the Scottish physician Alexander Fleming in 1928, however, common STIs have been underestimated adversaries for decades. In fact, such a “miracle drug” penicillin effectively rid society of grim visual reminders in the form of syphilitic facial deformities, allowing people to forget the sheer devastation caused by STIs. For almost a century now, humans have been misusing and overusing antibiotics,^{4,5} and, as a consequence, STIs—especially gonorrhea—are starting to develop antibiotic resistance, with potentially disastrous consequences for the treatment options.⁶ This is concerning, since over one million people are infected with a common STI every day,³ and the prevalence is rising: in 2019, the combined cases of gonorrhea, chlamydia and syphilis in the US rose to an all-time high for the sixth consecutive year.⁷ It appears that after a century of careless behavior with regard to antibiotics, STIs are coming back with a vengeance. Aggravating the problem is the COVID-19 pandemic, which, since its inception in January 2020, resulted in a disruption in STI services and a reallocation of resources,⁸ significantly reducing the number of visits to STI clinics.⁹ On the other hand, research studies have provided evidence that risky sexual behavior did not decrease during the government-mandated lockdowns and as a consequence of social distancing,¹⁰ thereby not reducing the risk of transmitting STIs. Since STIs are often asymptomatic or mildly symptomatic,¹¹ the reduction in visits to the clinic is problematic, and presents a peril in the possible escalation of a silent global pandemic, lurking in the shadows of the current COVID-19 health crisis. While condoms are very effective in preventing the spread of sexually transmitted diseases, they are used at varying degrees and risky sexual behavior is much too prevalent.¹² Hence, the current situation with STIs calls for a better understanding of the dynamics underlying the current trends of risky behavior and their impact on the spread of STIs, which could be key to help formulate and implement more effective control strategies.

Mathematical epidemic models on networks provide a powerful framework to represent and study the spread of infectious diseases in real-world populations.^{13–17} By analysing such models, the obtained insights can be used to inform control policies to aid in the eradication of the disease.^{14,17} In order to capture the real-world time-varying patterns of interactions between individuals, temporal networks are glowingly employed.^{17–19} Most of the literature on epidemic models focuses on air-borne infections,²⁰ for example, influenza viruses, SARS, and, more recently, great effort has been put toward successfully modeling COVID-19.^{21,22} In these models, the role of human behavior has often been overlooked or oversimplified, by assuming a priori an impact of human behavior on the model parameters (possibly identified using available data),²³ or by modeling a behavioral response governed by an awareness-driven reaction mechanism.^{24–26} However, since the spreading of STIs is directly linked to the sexual behavior of individuals, one should not readily assume that general epidemic models that neglect or simplify human behavior can adequately describe the spread of STIs. Some efforts have been made to propose network epidemic models tailored to represent the spreading of STIs. In Eames et al.,²⁷ a framework is introduced that deals with heterogeneity within contact networks. To study the effect of casual partners on the spread of STIs, a multilayer temporal network model is employed in Vajdi et al.²⁸ In Yan et al.,²⁹ a heterosexual contact network is modeled by employing a bipartite network. However, all these works do not explicitly take into account and model human behavioral preferences on the use of protections and how they change, limiting their applicability. Furthermore, the impact of control actions to mitigate the spread of STIs has often been oversimplified in the literature, for instance, by simply re-scaling the infection rate.²⁷

In this article, we propose a network model for the spreading of STIs that explicitly incorporates sexual behavioral tendencies and models their evolution. Specifically, we expand on the well-known stochastic susceptible–infected–susceptible (SIS) network model,¹⁷ used to model common STIs,³⁰ by adding further compartments to represent (i) individuals’ behavioral preferences with regard to the use of protection when engaging in sexual encounters; (ii) the presence of asymptomatic, unaware—but infectious—individuals; and (iii) treatment. Individual behavioral preferences are determined by the trade-off between the cost of using protection and the perceived risk (which depends on the detected infection prevalence), and it may also change due to an encounter with an individual having a different behavioral preference, who may be able to persuade the other individual to change their preferences. Sexual encounters are generated in a two-step probabilistic manner. First, an individual proposes a sexual encounter to another individual, according to a mechanism inspired by continuous-time activity-driven networks (ADNs), in which each individual initiates interactions with their peers in a stochastic fashion, yielding a time-varying pattern of social contacts.^{31,32} Specifically, the proposed mechanism takes into account the pattern of romantic relations in the population and the individuals’ tendency to cheat. Second, initiatives result in a sexual encounter according to a stochastic negotiation process, which accounts for the individuals’ level of complaisance during negotiation processes on the use of protection. In this article, we propose and study two different negotiation processes. Finally, we further incorporate three control measures

to impact the spread of infections: (i) condom (social) marketing campaigns, which have been shown through systematic studies to have a positive impact on the likelihood of the use of protective measures;³³ (ii) routine screening at STI clinics, determined to be most effective approach in controlling the spread of STIs;¹¹ and (iii) partner notification, known to be an effective method in detecting infected individuals.³⁴ Contact tracing of casual encounters comes with many challenges,³⁵ and patients themselves typically notify their romantic partners, but not their casual contacts,³⁶ so we let partner notification be restricted to romantic partners in this article. We will refer to our model as the behavioral SIS model.

In addition to the mathematical formulation of the behavioral SIS model, the main contributions of this article are twofold. First, we explicitly derive the epidemic threshold for the model, for two distinct negotiation processes on the use of protection, in the absence of a network of romantic relations and under some homogeneity assumptions on the model parameters. Our results, obtained through a mean-field analysis in the limit of large populations,³⁷ elucidate the role of routine screening and marketing campaigns in the spreading of STIs, and their effectiveness in controlling it. Specifically, we find that routine screening is key to combat the spreading of STIs, whereas marketing campaigns are only effective when combined with the former. Second, we perform numerical simulations to validate our theoretical findings and to extend them beyond the limitations of our analysis. Specifically, simulations are employed to examine the role of heterogeneity in the parameters, and to investigate the impact of partners on the epidemic spreading and the role of partner notification as a control measure. Our numerical findings suggest that homogeneous models can be good proxies for real-world systems, at least in the absence of partner networks, suggesting that our theoretical findings might be applied beyond the limitations of the homogeneity assumption. Furthermore, the analysis of the role of partners suggests that there is a nontrivial interplay between faithfulness and complaisance, depending on the negotiation process, while partner notification seems key to reduce the spread of STIs in faithful populations, suggesting that contact tracing for casual encounters might be a valuable additional measure to combat STIs.³⁴

Some preliminary results have appeared in Frieswijk et al.,³⁸ in which a similar extension of a behavioral SIS model was proposed, and the epidemic threshold was derived in two limiting cases. Here, we build on that preliminary effort and extend it along several directions. First, we expand the mathematical model with the inclusion of a network containing romantic partners and with a further control measure, that is, partner notification. Second, we consider an additional negotiation process, and examine its effect on the epidemic threshold. Third, we derive a general expression for the epidemic threshold, for both negotiation processes, which holds beyond the limiting cases analysed in the preliminary study. Fourth, we perform a campaign of numerical simulations of the model to further investigate its properties.

The rest of the article is organized as follows. After introducing some mathematical preliminaries and notation in Section 1.1, we formulate the mathematical model in Section 2. In Section 3, we derive the dynamical system that governs the network model. The theoretical results and simulations are presented in Section 4 and 5, respectively. Section 6 concludes our article and discusses future research avenues.

1.1 | Mathematical Preliminaries

Here, we gather the notational conventions used throughout the article, and we report some preliminary notions. The set of real, non-negative real, strictly positive real and non-negative integer numbers is denoted by \mathbb{R} , $\mathbb{R}_{\geq 0}$, $\mathbb{R}_{> 0}$ and $\mathbb{Z}_{\geq 0}$, respectively. Given two nodes j, k of a network, we denote by $\{j, k\}$ an undirected link between the nodes, and by (j, k) a directed link from j to k . Given a function $x(t)$ with $t \in \mathbb{R}_{\geq 0}$, we define $x(t^+) = \lim_{s \searrow t} x(s)$, and $x(t^-) = \lim_{s \nearrow t} x(s)$. Given an event E , we denote by $\mathbb{P}[E]$ its probability.

In the following, we provide the definitions of Poisson clocks and continuous-time Markov processes, and some important properties of Poisson clocks, which will be used throughout the article.

Definition 1 (Poisson clock³⁹). A Poisson clock with rate $\gamma \in \mathbb{R}_{\geq 0}$ is a continuous-time stochastic point process that can be represented by its counting process $N(t)$, which is a nondecreasing function that takes values in $\mathbb{Z}_{\geq 0}$. Specifically, the probability that the Poisson clock has an increment in a time step of duration $\Delta t \in \mathbb{R}_{> 0}$ is equal to

$$\mathbb{P}[N(t + \Delta t) - N(t) = 1] = \gamma \Delta t + o(\Delta t), \quad (1)$$

where the Landau little-o notation $o(\Delta t)$ is associated with the limit $\Delta t \searrow 0$; hence $\lim_{\Delta t \searrow 0} \mathbb{P}[N(t + \Delta t) - N(t) = 1]/\Delta t = \gamma$. If $N(t)$ has an increment at time $t \in \mathbb{R}_{\geq 0}$, we say that the clock *clicks* at time t .

Proposition 1 (Event triggered by Poisson clocks³⁹). *The following two properties hold true:*

- i) *Let E be an event that is associated with a set of Poisson clocks N_1, \dots, N_ℓ with rates $\gamma_1, \dots, \gamma_\ell$, respectively, each one independent of the others, and E occurs whenever one of the clocks in the set clicks. Then, we can equivalently describe the occurrences of event E as triggered by a Poisson clock N_E with rate equal to $\gamma_E := \sum_{h=1}^{\ell} \gamma_h$.*
- ii) *Let E be an event that is associated with a Poisson clock N with rate γ , and let E occur when the clock clicks with probability $p \in [0, 1]$, independent of the Poisson clock. Then, we can equivalently describe the occurrences of event E as triggered by a Poisson clock N_E with rate equal to $\gamma_E := p\gamma$.*

Definition 2 (Markov process⁴⁰). A continuous-time stochastic process $X(t)$ with the state space \mathcal{A} is a Markov process if, for any $h, k \in \mathcal{A}$, it holds that

$$\mathbb{P}[X(t + \Delta t) = k | X(t) = h] = \delta_{hk} + q_{hk}\Delta t + o(\Delta t), \quad (2)$$

where $q_{hk} \in \mathbb{R}_{\geq 0}$, for all $h \neq k \in \mathcal{A}$, is the *transition rate*. Furthermore, $q_{hh} := -\sum_{k \neq h} q_{hk}$, and

$$\delta_{hk} := \begin{cases} 1 & \text{if } h = k, \\ 0 & \text{if } h \neq k. \end{cases} \quad (3)$$

The transition rates are gathered in the *transition rate matrix* $Q \in \mathbb{R}^{|\mathcal{A}| \times |\mathcal{A}|}$.

From (2), it worth noticing that the transitions of a Markov process are regulated by Poisson clocks, each independent of the others. Hence, one can define a Markov process by defining all its transitions by means of independent Poisson clocks.

2 | MODEL

In this section, we will introduce the mathematical model. In Section 2.1, we introduce the network structure. Next, in Section 2.2, we discuss the modeling of sexual initiatives. Subsequently, we introduce the behavioral SIS model and the negotiation processes in Section 2.3, before moving on with the control parameters in Section 2.4.

2.1 | Population and partner network

We consider a population of n individuals $\mathcal{V} = \{1, \dots, n\}$. Each individual is represented by a node in a time-invariant undirected network $\mathcal{G}_P = (\mathcal{V}, \mathcal{E}_P)$, termed *partner network*. The edge set \mathcal{E}_P defines the partner relationships between individuals, so that $\{j, k\} \in \mathcal{E}_P$ if and only if j has a romantic relationship with k . In general, the partner network is not connected as it is formed by small-connected components. In fact, real-world partner networks are typically formed by pairs of nodes (steady couples) and isolated nodes (single individuals), but our modeling framework is flexible to capture more complex romantic relationships, for example, polyamorous relations, which have recently been estimated to be 4–5% of relations in the US.⁴¹ For each individual $j \in \mathcal{V}$, we define the set of partners of j as $\mathcal{P}_j := \{k \in \mathcal{V} : \{j, k\} \in \mathcal{E}_P\}$. Compared to the spreading of STIs, the partner network evolves at a much slower pace, so we make the simplifying assumption that \mathcal{E}_P is constant over time.

2.2 | Network of sexual initiatives

The STI may be transmitted from an infectious to a susceptible individual by means of an unprotected sexual encounter between the two individuals. Sexual encounters are modeled through a two-step stochastic mechanism. First, one individual makes a proposal to a second individual (to which we will refer as a *sexual initiative*), who in turn may or may not consider the proposal, as detailed below. Then, if the proposal is considered, it is accepted or rejected according to a negotiation process (detailed in Section 2.3), where it is assumed that romantic partner proposals are always considered

and accepted. In the first step, we generate a time-varying *directed* network of considered sexual initiatives $\mathcal{G}(t) = (\mathcal{V}, \mathcal{E}(t))$, with $t \in \mathbb{R}_{\geq 0}$, such that the directed edge $(j, k) \in \mathcal{E}(t)$ means that individual k considers a proposal made by individual j at time t .

In the following, we will detail the mechanism that generates sexual initiatives, which is inspired by continuous-time ADNs and acts as follows.³² Each individual j is equipped with a Poisson clock with unit rate, independent of the others. When a clock clicks, the individual associated to it activates and proposes a sexual encounter to another member of the population. Such a member is selected according to a stochastic mechanism. Specifically, to each $j \in \mathcal{V}$, we furthermore assign an individual-specific probability $p_j \in [0, 1]$, which represents the level of *faithfulness* to the partner relationship(s) of j , with the understanding that, if individual j is single ($\mathcal{P}_j = \emptyset$), then $p_j = 0$. Then, with probability p_j , individual j makes a proposal to one of their partners in \mathcal{P}_j (selected uniformly at random among them, if multiple partners are present); otherwise, with probability $1 - p_j$, the individual makes the proposal to a random individual in the rest of the population $k \in \mathcal{V} \setminus \{\mathcal{P}_j, j\}$, who considers the proposal with probability $1 - p_k$.

To sum up, the network formation process is encapsulated by the following algorithm.

- i) At time $t = 0$, initialize $\mathcal{E}(t) = \emptyset$.
- ii) If at time $t \in \mathbb{R}_{>0}$, the Poisson clock associated with individual $j \in \mathcal{V}$ ticks, then j activates and proposes a sexual encounter to another individual, which is selected as follows:
 - a) with probability p_j , individual j selects one of their romantic partners $k \in \mathcal{P}_j$ (chosen uniformly at random if j has multiple partners);
 - b) with probability $1 - p_j$, individual j initiates a casual encounter, where an individual $k \in \mathcal{V} \setminus \{j, \mathcal{P}_j\}$ is selected uniformly at random. Individual k considers a casual encounter with individual j with probability $1 - p_k$, or immediately declines the request with probability p_k .

If the sexual request of individual j is taken into consideration by k , then the ephemeral edge (j, k) is added to $\mathcal{E}(t)$.
- iii) Immediately afterwards, the Poisson clock associated with j is reset, $\mathcal{E}(t^+) = \emptyset$, and the algorithm resumes to step ii), from time t^+ .

Some illustrative examples of the network formation process are shown and discussed in Figure 1.

Remark 1. For the sake of simplicity, we make the assumption in this article that all the individuals activate with the same (unit) rate, which allows us to better focus on the role of the parameters that are related to the epidemic-behavioral model and to derive analytical results. However, heterogeneous tendencies to initiate sexual encounters can be easily incorporated within the modeling framework by assigning a parameter to each individual that determines the rate of the Poisson clock associated with their activation, similar to heterogeneous continuous-time activity driven networks,^{32,42} as proposed in our preliminary work.³⁸

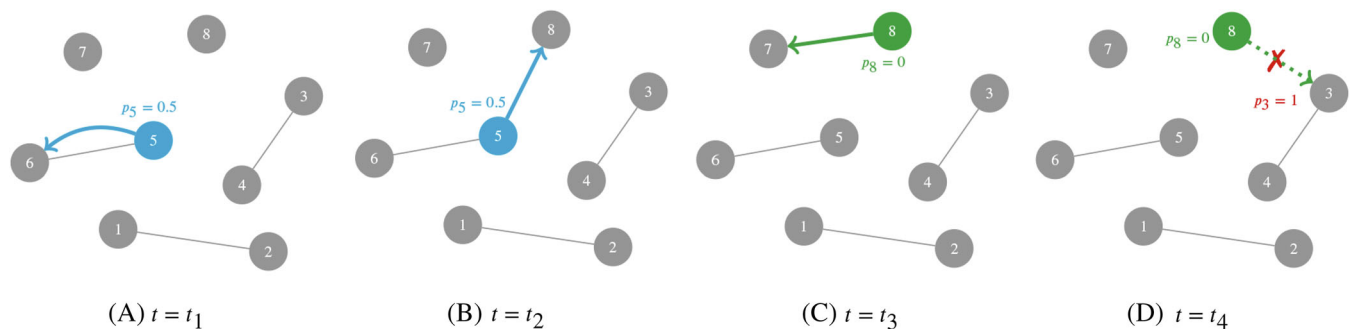


FIGURE 1 Example of four time-instances of the network of sexual initiatives $\mathcal{G}(t)$. The partner network \mathcal{G}_P is represented in gray. In (A), at time t_1 , the clock associated to 5 clicks; the node has faithfulness $p_5 = 0.5$ and, according to the stochastic mechanism, the individual proposes an encounter to the partner (node 6), so $(5, 6) \in \mathcal{E}(t_1)$. In (B), at time t_2 , the clock associated to node 5 clicks again; this time, the individual proposes an encounter to a random individual (8), who is single and always considers the proposal, so $(5, 8) \in \mathcal{E}(t_2)$. In (C), at time t_3 , the clock associated to 8 clicks; the individual is single ($p_8 = 0$), so they always makes a proposal to a random individual. The mechanism selects individual 7, who is single, so $(8, 7) \in \mathcal{E}(t_3)$. In (D), at time t_4 , the clock associated to 8 clicks again, and the individual proposes to 3. However, 3 has $p_3 = 1$ and turns down the proposal without even considering it. Hence, $\mathcal{E}(t_4) = \emptyset$

2.3 | Disease propagation and behavior

In this section, we present the epidemic model. In particular, we propose an extension of a classical network SIS model,^{16,17} in which we include additional compartments to account for detected infected individuals who are receiving treatment, and for behavioral preferences with regard to the use of protective measures during sexual encounters. We will refer to this model as the *behavioral SIS model*. As in Frieswijk et al.,³⁸ each individual $j \in \mathcal{V}$ is characterized by a state $X_j(t) \in \{S_r, S_p, I_r, I_p, I_t\}$, which reflects their *health state* and *behavioral preference* at time $t \in \mathbb{R}_{\geq 0}$. Specifically,

$$X_j(t) = \begin{cases} S_r & \text{if } j \text{ is } \textit{susceptible} \text{ and prefers to not use protective measures (} \textit{risky}), \\ S_p & \text{if } j \text{ is } \textit{susceptible} \text{ and prefers to use } \textit{protective} \text{ measures,} \\ I_r & \text{if } j \text{ is } \textit{infected}, \text{ unaware, and prefers to not use protective measures (} \textit{risky}), \\ I_p & \text{if } j \text{ is } \textit{infected}, \text{ unaware, and prefers to use } \textit{protective} \text{ measures,} \\ I_t & \text{if } j \text{ is } \textit{infected}, \text{ aware, and is receiving } \textit{treatment}, \end{cases}$$

at time t . We assume that treatment immediately follows if infected individuals become aware of their health status, either due to a positive screening result, or due to the development of symptoms. Here, we simplify matters by neglecting the possible time delay between the symptom onset and diagnosis, and between diagnosis and beginning of the treatment. Note that individuals who do not have symptoms—that is, susceptible and asymptomatic, infected individuals—display the same behavioral patterns, as long as they are unaware of their health state (so before screening takes place). States are gathered in the n -dimensional vector $X(t) = (X_1(t), \dots, X_n(t))$, which represents the system's state at time t .

STIs spread through pairwise encounters between infected and susceptible individuals, which occur in consonance with a mechanism detailed as follows. To each individual $j \in \mathcal{V}$, we assign a parameter $\sigma_j \in [0, 1]$, which represents individual j 's level of *compliance* in negotiation processes. Specifically, the parameter σ_j captures the deference of individual j to the wishes of others and the individual's willingness to please them. Hence, as σ_j increases, individual j will more likely accept to have a sexual encounter, regardless of their own behavioral preference. If $(j, k) \in \mathcal{E}(t)$, this means that at time t individual j makes a proposal to individual k , who considers the proposal. In this article, we will assume that individuals behave morally, which implies that individuals who are under treatment never propose or accept to have an unprotected intercourse. Hence, they never spread the STI. For the sake of simplicity, we can assume that if one of the individuals j and k is receiving treatment (i.e., $X_j(t) = I_t$ or $X_k(t) = I_t$), then a proposal is always rejected. If both j and k are not under treatment then, dependent on j 's behavioral inclination, j proposes to play risky (if $X_j(t) \in \{S_r, I_r\}$), or use protective measures (if $X_j(t) \in \{S_p, I_p\}$). Here, we assume that proposals from romantic partners are always accepted, whereas for casual encounters, the use of protection is decided by negotiation between the nonpartners. In this article, we investigate two different negotiation processes for casual encounters, which are detailed below.

1-stage negotiation process. When k considers a proposal made by $j \notin \mathcal{P}_k$ and the two individuals have the same behavioral preference, then k always accepts. If individual k 's behavioral preference differs, the proposal is accepted with probability σ_k , while the proposal is rejected with probability $1 - \sigma_k$ and no sexual encounter occurs. A schematic of this negotiation process is illustrated in Figure 2A.

2-stage negotiation process. When k considers a proposal made by $j \notin \mathcal{P}_k$, individual k always accepts if the two individuals have the same behavioral preference. Otherwise, the proposal is accepted with probability σ_k , whereas, with probability $1 - \sigma_k$, individual k makes a counter-proposal (according to their behavioral preference). Individual j subsequently accepts the counter-proposal with probability σ_j , or declines it with probability $1 - \sigma_j$. If j declines, no sexual encounter takes place. A schematic of this negotiation process is illustrated in Figure 2B.

If an individual accepts a proposal which conflicts with their original behavioral state (e.g., if an individual with a *risky* preference accepts a proposal from someone who prefers to use *protective* measures), then the behavioral preference of the individual changes accordingly (to a *protective* behavioral preference), consonant

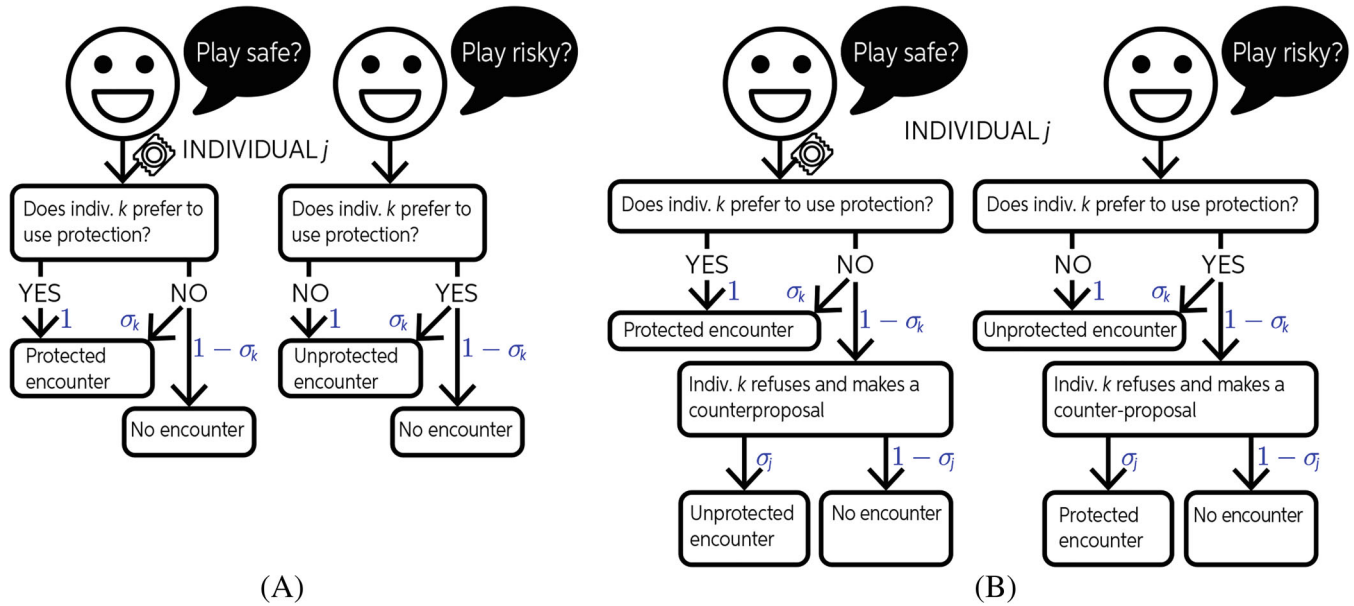


FIGURE 2 Flow chart of (A) a 1-stage negotiation process between nonpartners, and (B) a 2-stage negotiation process

with the literature on *decision inertia*, that is, people's penchant for repeating past decisions.^{43,44} The evolution of the state of an individual $j \in \mathcal{V}$ over time is described by the following processes and illustrated in Figure 3.

Behavioral changes due to persuasion. If a risky-minded individual ($X_j(t^-) \in \{S_r, I_r\}$) agrees to have a protected sexual encounter, then they switch to favoring the use of protection ($X_j(t^+) \in \{S_p, I_p\}$). Similarly, if an individual who favors the use of protective measures ($X_j(t^-) \in \{S_p, I_p\}$) agrees to have an unprotected sexual encounter, then they change to a risky-minded behavioral preference ($X_j(t^+) \in \{S_r, I_r\}$). Concurrently, a contagion may occur, detailed as follows.

Spontaneous rejection of protection. Besides the behavioral change due to a sexual encounter with a risky-minded individual, an individual with a protective preference ($X_j(t^-) \in \{S_p, I_p\}$) may spontaneously forego the will to protect ($X_j(t^+) \in \{S_r, I_r\}$) due to the cost of using protective measures, according to a Poisson clock with rate $c \in \mathbb{R}_{>0}$.

Epidemic fear. Apart from the behavioral change due to a sexual encounter with an individual who favors the use of protection, an individual with a risky behavioral tendency ($X_j(t^-) \in \{S_r, I_r\}$) may start to desire the use of protection ($X_j(t^+) \in \{S_p, I_p\}$) in response to epidemic spreading. Specifically, we define the detected infection prevalence at time t ,

$$I_t(t) := \frac{1}{n} \left| \{j \in \mathcal{V} : X_j(t) = I_t\} \right|, \quad (4)$$

and we model such a mechanism by employing a Poisson clock with a rate proportional to the detected prevalence, that is, when $I_t(t) = I_t$, we set the rate of the Poisson clock equal to ζI_t , where $\zeta \in \mathbb{R}_{\geq 0}$.

Contagion. If a susceptible individual ($X_j(t^-) \in \{S_r, S_p\}$) has an unprotected sexual encounter with an infected individual k ($X_k(t^-) \in \{I_r, I_p\}$), then j becomes infected ($X_j(t^+) = I_r$) with probability λ , where $\lambda \in [0, 1]$ is the *per-contact infection probability*.

Symptom onset. An asymptomatic infected individual ($X_j(t^-) \in \{I_r, I_p\}$) spontaneously develops symptoms and is diagnosed ($X_j(t^+) = I_t$) according to a Poisson clock with rate $\mu \in \mathbb{R}_{>0}$.

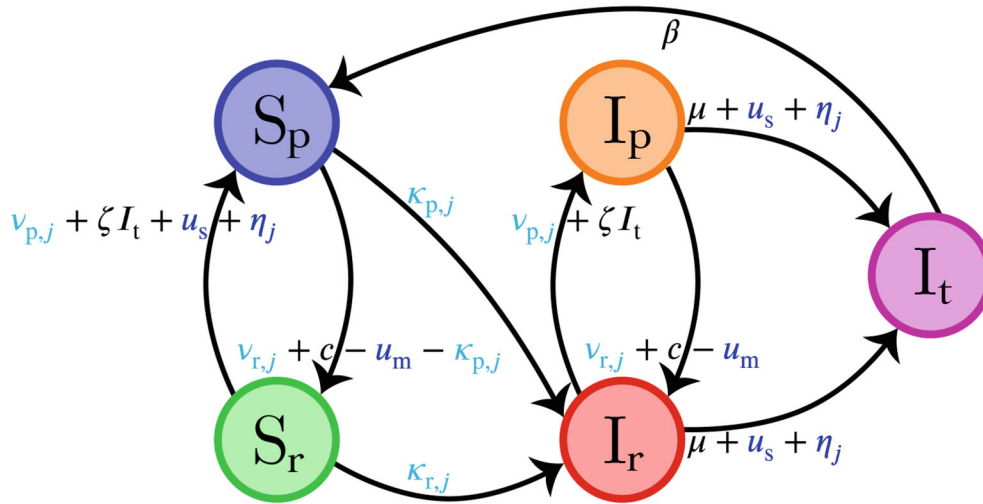


FIGURE 3 State transitions of the epidemic model for $j \in \mathcal{V}$. Rates in black refer to spontaneously triggered transitions, rates in cyan refer to transitions triggered by a sexual encounter (i.e., by pairwise interactions), and rates in blue refer to transitions driven by control actions

Recovery. An infected individual receiving treatment ($X_j(t^-) = I_t$) spontaneously recovers according to a Poisson clock with rate $\beta \in \mathbb{R}_{>0}$, as is typically assumed in stochastic epidemic models.^{14,17} We assume that after having recovered, j prefers to use protective measures ($X_j(t^+) = S_p$).

Remark 2. The model is amenable to several straightforward extensions. For instance, different costs for the individuals c_j can be set to capture heterogeneity in the population regarding the subjective cost of employing protective measures, which may be affected by social stigmas, prevailing moral norms, wealth status, and religious interdicts.⁴⁵ Moreover, more complex functions of the epidemic prevalence can be considered to model the epidemic fear, for example, to capture possible over-reacting or slow-to-react populations.⁴⁶

2.4 | Control parameters

Besides the spontaneous transition dynamics that regulate the epidemic-behavioral model, discussed in the previous section, we consider three control measures that may be implemented to mitigate the spreading of STIs.

Condom (social) marketing campaign. Social marketing programs induce individuals to employ protective measures during sexual encounters. The impact of such campaigns is implemented in the model by reducing the cost of using protection by $u_m \in [0, c]$, that is, by replacing c by $c - u_m$ in the “spontaneous rejection of protection” mechanism.

Routine screening at STI clinics. We investigate the impact of routine screening at STI clinics, and the distribution of free condoms after the test. By offering free STI screening, individuals who do not show symptoms are incentivized to undergo testing. Asymptomatic infected individuals ($X_j(t^-) \in \{I_r, I_p\}$) are diagnosed and treated ($X_j(t^+) = I_t$) according to a Poisson clock with rate $u_s \in \mathbb{R}_{\geq 0}$, representing the rate of routine screening. Susceptible individuals ($X_j(t^-) \in \{S_r, S_p\}$) may also undergo the same screening practices following a Poisson clock with rate u_s . After screening, we assume that susceptible individuals change their behavior to favoring the use of protective measures ($X_j(t^+) = S_p$), as they receive free condoms, and are moreover reminded of the perils of STIs.

TABLE 1 Notation and parameters of the behavioral SIS model

Symbol	Meaning	Symbol	Meaning
$X_j(t)$	State of individual j at time t	λ	Per-contact infection probability
\mathcal{P}_j	Set of partner(s) of j	μ	Rate of symptom onset
p_j	Faithfulness of j	β	Recovery rate
σ_j	Complaisance of j	u_m	Control effort in marketing campaign
c	Cost associated with protection	u_s	Control effort in screening campaign
ζ	Epidemic fear	u_n	Control effort in partner(s) notification

Partner notification. During the process of partner notification, romantic partners of a detected, infected individual k ($j \in \mathcal{P}_k : X_k(t^-) = I_t$) are contacted and informed of a potential exposure, and are requested to undergo screening. This measure is included in the modeling framework as follows. When $X(t) = (X_1, \dots, X_n)$, we define

$$\eta_j := u_n \left| \{k \in \mathcal{P}_j : X_k = I_t\} \right|, \quad (5)$$

where $u_n \in \mathbb{R}_{\geq 0}$ represents the enforcement level of partner notification. Depending on whether infection is detected among their romantic partner(s), individuals are tested according to a Poisson clock with rate η_j (in addition to the rate for routine screening). Note that η_j is proportional to the number of infected partners to account for multiple notifications, in accordance with Proposition 1. Similar to routine screening, after testing, infected individuals ($X_j(t^-) \in \{I_r, I_p\}$) are treated ($X_j(t^+) = I_t$), whereas susceptible individuals ($X_j(t^-) \in \{S_r, S_p\}$) change their behavioral preference to favoring the use of protective measures ($X_j(t^+) = S_p$).

All the parameters of the model are summarized in Table 1. Before presenting the details of the dynamical systems induced by these mechanisms, it is worth noticing that the model is characterized by sets of parameters that are clearly disentangled, and can thus be estimated independently, leaving few parameters to be identified from real-world epidemiological data. Such an important property will be key toward utilizing the proposed model in real-world scenarios, where the identification of many parameters from real-world data might be challenging or unfeasible.

In our model, in fact, the epidemic parameters λ , μ , and β are specific properties of the STI in consideration and are independent of human behavior. Hence, they can be calibrated from clinical and epidemiological data. The behavioral parameters p_j and σ_j , which determine an individual's faithfulness and complaisance, respectively, are characteristics of the population. Questionnaires and social surveys might be designed to estimate the distribution of these parameters in the population under analysis. The control parameters u_s and η_j are rates of Poisson clocks. Hence, their inverses are the average detection time of STIs via routine screening and partner notification, respectively, which characterize the effectiveness of these control measures. Finally, once all of these parameters are secured from clinical and sociological data, few parameters (i.e., the cost associated with protection c , the epidemic fear scalar ζ , and the control effort in marketing campaigns u_m) are left to be determined. These parameters, which are deeply related with the coevolution of an epidemic and behavior, might be then identified from real-world data on the diffusion of STIs and on the use of protective measures.

3 | DYNAMICS

In this section, we will present the details of the dynamical systems induced by the mechanisms described in the previous section. First, we observe that all the mechanisms in the model are triggered by Poisson clocks, each one independent of the others. Hence, in view of the observations made in Section 1.1, the system's state $X(t)$ evolves according to a continuous-time n -dimensional Markov process in the state space $\{S_r, S_p, I_r, I_p, I_t\}^n$. As illustrated in Figure 3, the generic

j th entry of the vector $X(t)$ can undergo nine different state transitions. Three of them—namely, the ones from I_p and I_r to I_t , and the one from I_t to S_p —are just triggered by spontaneous mechanisms, and the corresponding transition rates are simply equal to the sum of the rates of the Poisson clocks involved in the process, in accordance with Proposition 1. Hence, we obtain that:

- the transition rate from I_r to I_t is equal to the sum of the symptom onset rate μ , the control effort placed in routine screening u_s , and the partner notification η_j ;
- the transition rate from I_p to I_t is equal to the above, that is, $\mu + u_s + \eta_j$; and
- the transition rate from I_t to S_p is equal to β .

The other six transitions, on the other hand, involve mechanisms that are triggered by interactions between individuals. These mechanisms are the contagion process (which may occur when a susceptible individual has an unprotected encounter with an infected individuals) and the behavioral changes due to persuasion (which occur when an individual accepts an encounter in conflict with their behavioral preference). For a generic individual j , we denote by $\kappa_{p,j}$ and $\kappa_{r,j}$ the rate corresponding to their contagion process if they have a protective or risky behavioral preference, respectively, and by $v_{p,j}$ and $v_{r,j}$ the rate of the persuasion process to a protective and risky preference, respectively. The explicit expressions for these rates depend on the nature of the negotiation process; the expressions for the two negotiation processes considered in this article are derived below.

Similar to the other three rates, we derive the expression for the overall transition rate from one state to another by summing all the rates of the mechanisms that may trigger the transition, in accordance with Proposition 1, which gives that:

- the transition rate from S_r to I_r is equal to the contagion rate $\kappa_{r,j}$;
- the transition rate from S_p to I_r is equal to the contagion rate $\kappa_{p,j}$;
- the transition rate from S_r to S_p is equal to the sum of the persuasion effect $v_{p,j}$, the risk perception ζI_t , the control effort placed in routine screening u_s , and partner notification η_j ;
- the transition rate from I_r to I_p is equal to the sum of the persuasion effect $v_{p,j}$ and the risk perception ζI_t (since an infected individual that undergoes screening would test positive and transition to the diagnosed compartment I_t);
- the transition rate from I_p to I_r is equal to the sum of the persuasion effect $v_{r,j}$ and the cost of using protective measures minus the control effort placed in marketing campaigns $c - u_m$;
- the transition rate from S_p to S_r is equal to the one above, reduced by $\kappa_{p,j}$ due to contagion taking place. Hence, it is equal to $v_{r,j} + c - u_m - \kappa_{p,j}$.

To sum up, the nine rates described above can be gathered into the transition rate matrix for the generic j th component of the Markov process $X(t)$ as

$$Q_j = \begin{bmatrix} \cdot & v_{p,j} + \zeta I_t + u_s + \eta_j & \kappa_{r,j} & 0 & 0 \\ v_{r,j} + c - u_m - \kappa_{p,j} & \cdot & \kappa_{p,j} & 0 & 0 \\ 0 & 0 & \cdot & v_{p,j} + \zeta I_t & \mu + u_s + \eta_j \\ 0 & 0 & v_{r,j} + c - u_m & \cdot & \mu + u_s + \eta_j \\ 0 & \beta & 0 & 0 & \cdot \end{bmatrix}, \tag{6}$$

where the rows (columns) correspond to state S_r, S_p, I_r, I_p , and I_t , respectively. The diagonal elements equal the opposite of the sum of the other elements of the row, so each row of Q_j sums to zero. Hence, following Definition 2, for any $h, k \in \{S_r, S_p, I_r, I_p, I_t\}$ with $h \neq k$,

$$\mathbb{P} [X_j(t + \Delta t) = k | X_j(t) = h] = (Q_j)_{hk} \Delta t + o(\Delta t). \tag{7}$$

In the following subsections, we explicitly derive the expressions for the contagion and the persuasion rates, for the 1-stage and the 2-stage negotiation process.

3.1 | The 1-stage negotiation process

For the 1-stage negotiation process, we derive the following expressions for the rates associated with contagion and persuasion.

Contagion. If $X_j(t^-) = S_r$, then j can contract the disease ($X_j(t^+) = I_r$). Specifically, this happens if one of the following events occurs: (i) j proposes an encounter to an infected partner (recalling that partners always accept proposals); (ii) j proposes an encounter to an infected nonpartner who has a preference for risky behavior; (iii) j proposes an encounter to an infected nonpartner who prefers to use protection, but j persuades the nonpartner to have an unprotected encounter; (iv) a partner of j who has a preference for risky behavior proposes an encounter to j ; or (v) someone who is not a partner of j and has a preference for risky behavior proposes an encounter to j . Hence, in accordance with Proposition 1, contagion occurs according to a Poisson clock with rate equal to the sum of the rates of the five possible events described above, multiplied by the per-contact infection probability λ , which yields

$$\begin{aligned} \kappa_{r,j} = \kappa_{r,j}^{(1)} := & \lambda \left(\frac{p_j}{|\mathcal{P}_j|} \sum_{\substack{k \in \mathcal{P}_j: \\ X_k \in \{I_r, I_p\}}} 1 + \frac{1-p_j}{n-1-|\mathcal{P}_j|} \left[\sum_{\substack{k \in \mathcal{V} \setminus \{\mathcal{P}_j\}: \\ X_k = I_r}} (1-p_k) + \sum_{\substack{k \in \mathcal{V} \setminus \{\mathcal{P}_j\}: \\ X_k = I_p}} (1-p_k)\sigma_k \right] \right) \\ & + \lambda \left(\sum_{\substack{k \in \mathcal{P}_j: \\ X_k = I_r}} \frac{p_k}{|\mathcal{P}_k|} + (1-p_j) \sum_{\substack{k \in \mathcal{V} \setminus \{\mathcal{P}_j\}: \\ X_k = I_r}} \frac{1-p_k}{n-1-|\mathcal{P}_k|} \right), \end{aligned} \quad (8)$$

with the convention (kept throughout the article) that sums over empty sets are omitted. If $X_j(t^-) = S_p$, individual j can also become infected ($X_j(t^+) = I_r$). In particular, this happens if one of the following events occurs: (i) a partner of j who has a preference for risky behavior proposes an encounter to j , who always accepts; or (ii) someone who is not a partner of j and has a preference for a risky behavior proposes an encounter to j , who is persuaded. Hence, in accordance with Proposition 1, contagion occurs according to a Poisson clock with rate equal to the sum of the rates of the two possible events described above, multiplied by the per-contact infection probability λ , yielding

$$\kappa_{p,j} = \kappa_{p,j}^{(1)} := \lambda \left(\sum_{\substack{k \in \mathcal{P}_j: \\ X_k = I_r}} \frac{p_k}{|\mathcal{P}_k|} + (1-p_j)\sigma_j \sum_{\substack{k \in \mathcal{V} \setminus \{\mathcal{P}_j\}: \\ X_k = I_r}} \frac{1-p_k}{n-1-|\mathcal{P}_k|} \right). \quad (9)$$

Persuasion. If $X_j(t) \in \{S_p, I_p\}$, j can stop favoring the use of protective measures ($X_j(t^+) \in \{S_r, I_r\}$). This occurs if j is persuaded by a proposal from a risky-minded individual (partner or nonpartner). Recalling that proposals from partners are always accepted and using Proposition 1, this happens according to a Poisson clock with rate

$$v_{r,j} = v_{r,j}^{(1)} := \sum_{\substack{k \in \mathcal{P}_j: \\ X_k \in \{S_r, I_r\}}} \frac{p_k}{|\mathcal{P}_k|} + (1-p_j)\sigma_j \sum_{\substack{k \in \mathcal{V} \setminus \{\mathcal{P}_j\}: \\ X_k \in \{S_r, I_r\}}} \frac{1-p_k}{n-1-|\mathcal{P}_k|}. \quad (10)$$

If $X_j(t^-) \in \{S_r, I_r\}$, j can start to desire the use of protection ($X_j(t^+) \in \{S_p, I_p\}$). This happens if j is persuaded by a proposal of someone (partner or nonpartner) who has a preference for using protective measures. Recalling that proposals from partners are always accepted and using Proposition 1, this happens according to a Poisson clock with rate

$$v_{p,j} = v_{p,j}^{(1)} := \sum_{\substack{k \in \mathcal{P}_j: \\ X_k \in \{S_p, I_p\}}} \frac{p_k}{|\mathcal{P}_k|} + (1-p_j)\sigma_j \sum_{\substack{k \in \mathcal{V} \setminus \{\mathcal{P}_j\}: \\ X_k \in \{S_p, I_p\}}} \frac{1-p_k}{n-1-|\mathcal{P}_k|}. \quad (11)$$

3.2 | The 2-stage negotiation process

For the 2-stage negotiation process, individuals make a counter-proposal if they decline the original proposal. As a result, contagion and persuasion may occur in all the events listed for the 1-stage negotiation process (see Section 3.1), but also upon acceptance of counter-proposals. Hence, according to Proposition 1, the corresponding rates are augmented by an additional term that accounts for the acceptance of a counter-proposal by a nonpartner, while partners always accept the proposal (so no counter-proposal will be made). Hence, we summarize the rates as follows.

Contagion. If $X_j(t^-) = S_r, j$ gets infected ($X_j(t^+) = I_r$) according to a Poisson clock with rate

$$\kappa_{r,j} = \kappa_{r,j}^{(2)} := \kappa_{r,j}^{(1)} + \lambda(1 - p_j)(1 - \sigma_j) \sum_{\substack{k \in \mathcal{V} \setminus \{\mathcal{P}_j\} \\ X_k = I_p}} \frac{\sigma_k(1 - p_k)}{n - 1 - |\mathcal{P}_j|}. \tag{12}$$

If $X_j(t^-) = S_p$, individual j contracts the disease ($X_j(t^+) = I_r$) following a Poisson clock with rate

$$\kappa_{p,j} = \kappa_{p,j}^{(2)} := \kappa_{p,j}^{(1)} + \lambda \sigma_j \frac{1 - p_j}{n - 1 - |\mathcal{P}_j|} \sum_{\substack{k \in \mathcal{V} \setminus \{\mathcal{P}_j\} \\ X_k = I_r}} (1 - p_k)(1 - \sigma_k). \tag{13}$$

Persuasion. If $X_j(t) \in \{S_p, I_p\}$, j is persuaded to no longer desire the use of protection ($X_j(t^+) \in \{S_r, I_r\}$) according to a Poisson clock with rate

$$v_{r,j} = v_{r,j}^{(2)} := v_{r,j}^{(1)} + \sigma_j \frac{1 - p_j}{n - 1 - |\mathcal{P}_j|} \sum_{\substack{k \in \mathcal{V} \setminus \{\mathcal{P}_j\} \\ X_k \in \{S_r, I_r\}}} (1 - p_k)(1 - \sigma_k). \tag{14}$$

If $X_j(t^-) \in \{S_r, I_r\}$, j is persuaded to start desiring the use of protective measures ($X_j(t^+) \in \{S_p, I_p\}$) according to a Poisson clock with rate

$$v_{p,j} = v_{p,j}^{(2)} := v_{p,j}^{(1)} + \sigma_j \frac{1 - p_j}{n - 1 - |\mathcal{P}_j|} \sum_{\substack{k \in \mathcal{V} \setminus \{\mathcal{P}_j\} \\ X_k \in \{S_p, I_p\}}} (1 - p_k)(1 - \sigma_k). \tag{15}$$

Now, we are ready to present our main results in the following section.

4 | MAIN RESULTS

In this section, we derive some analytical insight into the system. Specifically, we focus on the computation of the epidemic threshold of the model for the two negotiation processes. The epidemic threshold determines a region in the parameter space in which local outbreaks are always quickly eradicated and never give rise to global pandemics.

We start our analysis by observing that the transition matrix for individual j defined in (6) is dependent on the state of the other individuals. This complicates the direct analysis of the Markov process $X(t)$ for large-scale populations, since the nodal dynamics cannot be decoupled, and as a consequence, the dimension of the state space of the system grows exponentially with n . Hence, as often done in the literature,^{37,47} we rely on a continuous-state deterministic mean-field relaxation of the stochastic system, which approximates the evolution of the stochastic system in the thermodynamic limit of large-scale populations $n \rightarrow \infty$. Specifically, for all individuals $j \in \mathcal{V}$, we define the following five probabilities:

$$\begin{aligned} s_{r,j}(t) &:= \mathbb{P} [X_j(t) = S_r], & s_{p,j}(t) &:= \mathbb{P} [X_j(t) = S_p], & i_{r,j}(t) &:= \mathbb{P} [X_j(t) = I_r], \\ i_{p,j}(t) &:= \mathbb{P} [X_j(t) = I_p], & i_{t,j}(t) &:= \mathbb{P} [X_j(t) = I_t], \end{aligned} \tag{16}$$

that is, the probability that individual j is in each of the five states at time t . The mean-field relaxation³⁷ consists of the study of a system of $5n$ ordinary differential equations (ODEs) that governs the evolution of the variables defined in (16), for all $j \in \mathcal{V}$. These ODEs are derived as $(\dot{s}_{r,j} \dot{s}_{p,j} \dot{i}_{r,j} \dot{i}_{p,j} \dot{i}_{t,j}) = (s_{r,j} s_{p,j} i_{r,j} i_{p,j} i_{t,j}) \tilde{Q}_j$, where \tilde{Q}_j is the mean-field expression of the transition rate matrix in (6), which is obtained by substituting the indicator functions in the sums in $\kappa_{r,j}$, $\kappa_{p,j}$, $\nu_{r,j}$, and $\nu_{p,j}$ with the corresponding probabilities defined in (16), obtaining the mean-field expressions $\tilde{\kappa}_{r,j}$, $\tilde{\kappa}_{p,j}$, $\tilde{\nu}_{r,j}$, and $\tilde{\nu}_{p,j}$, respectively (see Appendix A for more details and their explicit derivations). Such a procedure leads to the following result.

Proposition 2. *The mean-field evolution of the behavioral SIS model $X(t)$ defined in (6) is governed by the following system:*

$$\begin{aligned}\dot{s}_{r,j} &= - \left(\tilde{\nu}_{p,j} + u_s + \zeta \frac{1}{n} \sum_{k \in \mathcal{V}} \dot{i}_{t,k} + \eta_j + \tilde{\kappa}_{r,j} \right) s_{r,j} + (\tilde{\nu}_{r,j} + c - u_m - \tilde{\kappa}_{p,j}) s_{p,j}, \\ \dot{s}_{p,j} &= \left(\tilde{\nu}_{p,j} + u_s + \zeta \frac{1}{n} \sum_{k \in \mathcal{V}} \dot{i}_{t,k} + \eta_j \right) s_{r,j} - (\tilde{\nu}_{r,j} + c - u_m) s_{p,j} + \beta \dot{i}_{t,j}, \\ \dot{i}_{r,j} &= \tilde{\kappa}_{r,j} s_{r,j} + \tilde{\kappa}_{p,j} s_{p,j} - \left(\tilde{\nu}_{p,j} + \zeta \frac{1}{n} \sum_{k \in \mathcal{V}} \dot{i}_{t,k} + \mu + u_s + \eta_j \right) i_{r,j} + (\tilde{\nu}_{r,j} + c - u_m) i_{p,j}, \\ \dot{i}_{p,j} &= \left(\tilde{\nu}_{p,j} + \zeta \frac{1}{n} \sum_{k \in \mathcal{V}} \dot{i}_{t,k} \right) i_{r,j} - (\tilde{\nu}_{r,j} + c - u_m + \mu + u_s + \eta_j) i_{p,j}, \\ \dot{i}_{t,j} &= (\mu + u_s + \eta_j) i_{r,j} + (\mu + u_s + \eta_j) i_{p,j} - \beta \dot{i}_{t,j},\end{aligned}\quad (17)$$

for all $j \in \mathcal{V}$, where the explicit expressions of the mean-field transition rates $\tilde{\kappa}_{r,j}$, $\tilde{\kappa}_{p,j}$, $\tilde{\nu}_{r,j}$, and $\tilde{\nu}_{p,j}$ are reported in Appendix A.

In order to perform the numerical and theoretical analysis of system (17), we will first show that the system is well-defined, that is, that $(s_{r,j}(t) s_{p,j}(t) i_{r,j}(t) i_{p,j}(t) i_{t,j}(t))$ governed by (17) forms a probability vector for all $j \in \mathcal{V}$, and for all $t \in \mathbb{R}_{\geq 0}$.

Lemma 1. *The set $\{(s_{r,j} s_{p,j} i_{r,j} i_{p,j} i_{t,j}) : s_{r,j}, s_{p,j}, i_{r,j}, i_{p,j}, i_{t,j} \geq 0, s_{r,j} + s_{p,j} + i_{r,j} + i_{p,j} + i_{t,j} = 1\}$ is positive invariant under (17), for all $j \in \mathcal{V}$.*

Proof. From (17), we immediately observe that $\dot{s}_{r,j} + \dot{s}_{p,j} + \dot{i}_{r,j} + \dot{i}_{p,j} + \dot{i}_{t,j} = 0$, for all $j \in \mathcal{V}$. If the initial condition is well-defined, then necessarily $s_{r,j} + s_{p,j} + i_{r,j} + i_{p,j} + i_{t,j} = 1$ for all $t \in \mathbb{R}_{\geq 0}$. Finally, we observe that if one of the probabilities governed by (17) is equal to zero, then its time-derivative is always non-negative. Thus, $s_{r,j}, s_{p,j}, i_{r,j}, i_{p,j}, i_{t,j} \geq 0$ for all $t \in \mathbb{R}_{\geq 0}$. ■

It follows from Lemma 1 that system (17) consists of $4n$ linearly independent differential equations, which will be useful to simplify the computations in the next section.

Before stating our results, let us introduce some more notation. We define five macroscopic quantities that measure the average probability for a randomly selected individual to be in state S_r , S_p , I_r , I_p , and I_t as

$$y_{s,r} := \frac{1}{n} \sum_{j \in \mathcal{V}} s_{r,j}, \quad y_{s,p} := \frac{1}{n} \sum_{j \in \mathcal{V}} s_{p,j}, \quad y_{i,r} := \frac{1}{n} \sum_{j \in \mathcal{V}} i_{r,j}, \quad y_{i,p} := \frac{1}{n} \sum_{j \in \mathcal{V}} i_{p,j}, \quad \text{and} \quad y_{i,t} := \frac{1}{n} \sum_{j \in \mathcal{V}} i_{t,j}, \quad (18)$$

respectively. The relation between the original stochastic system defined through the transition matrix (6) and its mean-field approximation is now discussed. For a sufficiently large enough population size n , the prevalence of the states can be arbitrarily closely approximated by (18) for any finite time-horizon,^{42,48} that is,

$$\begin{aligned}S_r(t) &:= \frac{1}{n} |\{j \in \mathcal{V} : X_j(t) = S_r\}| \approx y_{s,r}, & S_p(t) &:= \frac{1}{n} |\{j \in \mathcal{V} : X_j(t) = S_p\}| \approx y_{s,p}, \\ I_p(t) &:= \frac{1}{n} |\{j \in \mathcal{V} : X_j(t) = I_p\}| \approx y_{i,p}, & I_r(t) &:= \frac{1}{n} |\{j \in \mathcal{V} : X_j(t) = I_r\}| \approx y_{i,r},\end{aligned}$$

and $I_t(t) \approx y_{i,t}$. Figure 4 shows the accuracy of this approximation in the scenario of a 1-stage negotiation process (detailed in the following subsection) as the population size n grows large. Hence, even though the mean-field approximation may

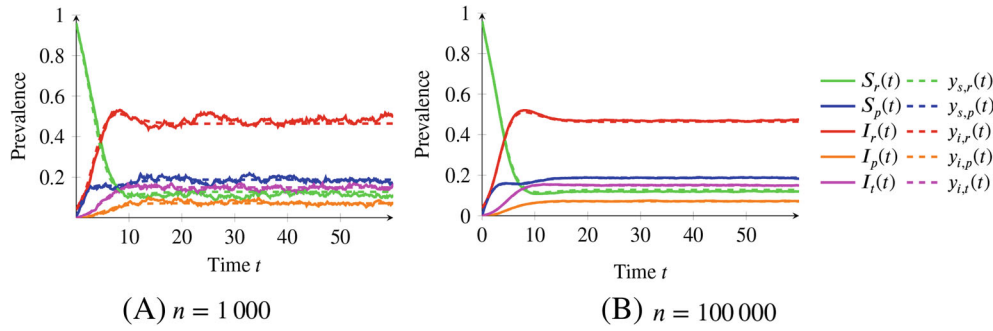


FIGURE 4 Simulations of the behavioral SIS model (solid curves) and its deterministic approximation (dashed curves) for population size (A) $n = 1\,000$; and (B) $n = 100\,000$. The model parameters are $\lambda = 0.5$, $u_s = 0.1$, $c = 0.4$, $u_m = 0.1$, $\mu = 0.04$, $\zeta = 1$, $\beta = 0.5$, and $\sigma_j = 0.4$, for all $j \in \mathcal{V}$. In both simulations, we have utilized the 1-stage negotiation process, and we have assumed that there is no partner network

not be able to accurately predict the individual-level behavior, it allows to precisely reproduce the emergent behavior of the system at the level of the macroscopic variables, providing a tool to determine whether an epidemic outbreak will be quickly eradicated or if it will spread in the population.

Due to the complexity of the dynamics and the large number of parameters involved in the model, the analytical computation of the threshold is in general unfeasible. Here, we derive its analytical expression under some simplifying assumptions, that is, by assuming a population with homogeneous complaisance $\sigma_j = \sigma$, for all $j \in \mathcal{V}$, and by neglecting the partner backbone. Numerical simulations will be employed to extend our findings beyond these limitations. Hence, for the rest of this section, we will consider the system under the following assumption.

Assumption 1. We assume that $\mathcal{P}_j = \emptyset$ and $\sigma_j = \sigma \in [0, 1]$, for all $j \in \mathcal{V}$.

In Sections 4.1 and 4.2, we will derive the explicit expressions of the mean-field equations for the 1-stage and the 2-stage negotiation process, respectively, and subsequently use them to derive the epidemic threshold for the two scenarios.

4.1 | The 1-stage negotiation process

In this section, we derive the epidemic threshold for our behavioral SIS model, under the 1-stage negotiation process, to shed light on the impact of condom (social) marketing campaigns and routine screening on the spreading of STIs. We achieve this by taking the mean-field relaxation, resulting in the following proposition, which is obtained from Proposition 2, by substituting the mean-field expressions of (8)–(11), which are reported in Appendix A, into (17). Explicit computations are straightforward, so we can safely omit them here and report the final result. For the sake of completeness, the proof of Proposition 3 is reported in Appendix B.

Proposition 3. Under Assumption 1 and with the 1-stage negotiation process, the mean-field evolution of the behavioral SIS model follows

$$\begin{aligned}
 \dot{s}_{r,j} &= - \left(\gamma_{p,j} + u_s + \zeta \frac{1}{n} \sum_{k \in \mathcal{V}} i_{t,k} + \frac{\lambda}{n-1} \sum_{k \in \mathcal{V} \setminus \{j\}} (2i_{r,k} + \sigma i_{p,k}) \right) s_{r,j} + \left(\gamma_{r,j} + c - u_m - \frac{\lambda \sigma}{n-1} \sum_{k \in \mathcal{V} \setminus \{j\}} i_{r,k} \right) s_{p,j}, \\
 \dot{s}_{p,j} &= \left(\gamma_{p,j} + u_s + \zeta \frac{1}{n} \sum_{k \in \mathcal{V}} i_{t,k} \right) s_{r,j} - (\gamma_{r,j} + c - u_m) s_{p,j} + \beta i_{t,j}, \\
 \dot{i}_{r,j} &= \left(\frac{\lambda}{n-1} \sum_{k \in \mathcal{V} \setminus \{j\}} (2i_{r,k} + \sigma i_{p,k}) \right) s_{r,j} + \left(\frac{\lambda \sigma}{n-1} \sum_{k \in \mathcal{V} \setminus \{j\}} i_{r,k} \right) s_{p,j} - \left(\gamma_{p,j} + \zeta \frac{1}{n} \sum_{k \in \mathcal{V}} i_{t,k} + \mu + u_s \right) i_{r,j} + (\gamma_{r,j} + c - u_m) i_{p,j}, \\
 \dot{i}_{p,j} &= \left(\gamma_{p,j} + \zeta \frac{1}{n} \sum_{k \in \mathcal{V}} i_{t,k} \right) i_{r,j} - (\gamma_{r,j} + c - u_m + \mu + u_s) i_{p,j}, \\
 \dot{i}_{t,j} &= (\mu + u_s) i_{r,j} + (\mu + u_s) i_{p,j} - \beta i_{t,j},
 \end{aligned} \tag{19}$$

for all $j \in \mathcal{V}$, where we define

$$\gamma_{r,j} := \frac{\sigma}{n-1} \sum_{k \in \mathcal{V} \setminus \{j\}} (s_{r,k} + i_{r,k}), \quad \text{and} \quad \gamma_{p,j} := \frac{\sigma}{n-1} \sum_{k \in \mathcal{V} \setminus \{j\}} (s_{p,k} + i_{p,k}). \quad (20)$$

In view of the above, we will use the macroscopic variables defined in (18) to study the behavior of large populations. Specifically, we aspire to determine whether there exist conditions that prevent the escalation of a local outbreak of the disease into an endemic situation. Formally, we aim to obtain the necessary condition(s) for the existence of a (locally) asymptotically stable disease-free equilibrium. In the following theorem, we present this condition, that is, the *epidemic threshold*, for system (19). Here, the threshold is presented as a critical value of the parameter μ . If the rate of symptom onset μ is higher than the critical value μ^* , then the outbreak is quickly eradicated; if not, it becomes endemic. Note that $\mu \in \mathbb{R}_{>0}$, so for any negative value of μ^* , eradication of the outbreak is guaranteed.

Theorem 1. Consider the behavioral SIS model for a 1-stage negotiation process under Assumption 1, given by (19), in the limit $n \rightarrow \infty$. Then, the system has a unique disease-free equilibrium (with $y_{i,r} = y_{i,p} = y_{i,t} = 0$), which is locally asymptotically stable if and only if

$$\mu > \mu_1^* := -\frac{1}{2}\sigma - \frac{1}{2(u_s + c - u_m)} \left[2u_s^2 + (c - u_m)^2 + (c - u_m)(3u_s - 2\lambda) - \lambda\sigma u_s - \sqrt{v_1} \right], \quad (21)$$

where

$$v_1 := (c - u_m)^4 + 2(c - u_m)^3 [2\lambda + \sigma + u_s] + (c - u_m)^2 [\sigma^2 + (2\lambda + u_s)^2 + 2\sigma(2\lambda + u_s(\lambda + 2))] + 2\sigma u_s(c - u_m) [2\lambda^2 + \lambda(u_s + 3\sigma - 2) + \sigma + u_s] + \sigma^2 u_s^2 (\lambda - 1)^2. \quad (22)$$

Proof. First, it can be observed from (19) that there is a unique disease-free equilibrium with $y_{i,r} = y_{i,p} = y_{i,t} = 0$, which is given by

$$(s_{r,j}, s_{p,j}, i_{r,j}, i_{p,j}, i_{t,j}) = \left(\frac{c - u_m}{u_s + c - u_m}, \frac{u_s}{u_s + c - u_m}, 0, 0, 0 \right), \quad (23)$$

for all $j \in \mathcal{V}$. Equilibrium (23) is always globally asymptotically stable when restricting the dynamics to the disease-free manifold $i_{r,j} = i_{p,j} = i_{t,j} = 0$ for all $j \in \mathcal{V}$. To study its local stability, instead of directly studying the system of $4n$ linearly independent equations for the individual-level variables (16) in (19), we utilize the macroscopic variables defined in (18), observing that the disease-free equilibrium is stable if and only if $\left(\frac{c - u_m}{u_s + c - u_m}, \frac{u_s}{u_s + c - u_m}, 0, 0, 0 \right)$ is a stable equilibrium for the system of macroscopic variables. For the sake of readability, we define a change of variables, where the macroscopic variable $y_{s,p}$ is substituted by the auxiliary variable

$$y_q := \frac{1}{n} \sum_{j \in \mathcal{V}} \left(s_{p,j} - \frac{u_s}{u_s + c - u_m} \right) = y_{s,p} - \frac{u_s}{u_s + c - u_m}, \quad (24)$$

while we choose to omit variable $y_{s,r}$ (as a consequence of Lemma 1), since is not independent of the other four macroscopic variables. Note that, in the new system of four variables, the disease-free equilibrium coincides with the origin. Substituting system (19) into (18) and (24), and subsequently linearising the result about the disease-free equilibrium (i.e., the origin in the new system of variables $y_q, y_{i,r}, y_{i,p}$, and $y_{i,t}$), gives the following linearly independent system:

$$\begin{aligned} \dot{y}_q = & -(u_s + c - u_m)y_q - \left(\sigma \frac{u_s}{u_s + c - u_m} + u_s \right) y_{i,r} + \left(\sigma \left(1 - \frac{u_s}{u_s + c - u_m} \right) - u_s \right) y_{i,p} \\ & + \left(\zeta \left(1 - \frac{u_s}{u_s + c - u_m} \right) + \beta - u_s \right) y_{i,t}, \end{aligned}$$

$$\begin{aligned}
 \dot{y}_{i,r} &= \left((\lambda\sigma - 2\lambda - \sigma) \frac{u_s}{u_s + c - u_m} + 2\lambda - u_s - \mu \right) y_{i,r} + \left(\sigma(\lambda + 1) \left(1 - \frac{u_s}{u_s + c - u_m} \right) + c - u_m \right) y_{i,p}, \\
 \dot{y}_{i,p} &= \sigma \frac{u_s}{u_s + c - u_m} y_{i,r} - \left(\sigma \left(1 - \frac{u_s}{u_s + c - u_m} \right) + c - u_m + \mu + u_s \right) y_{i,p}, \\
 \dot{y}_{i,t} &= (\mu + u_s) y_{i,r} + (\mu + u_s) y_{i,p} - \beta y_{i,t}.
 \end{aligned}
 \tag{25}$$

Equilibrium (23) is (locally) asymptotically stable for (19) if and only if the origin is (locally) asymptotically stable under (25). From (25), we explicitly compute the eigenvalues of the Jacobian matrix, obtaining two terms that are always negative, $-(u_s + c - u_m) < 0$ and $-\beta < 0$, and

$$-\mu - \frac{1}{2}\sigma - \frac{1}{2(u_s + c - u_m)} \left[2u_s^2 + (c - u_m)^2 + (c - u_m)(3u_s - 2\lambda) - \lambda\sigma u_s \pm \sqrt{v_1} \right],
 \tag{26}$$

where v_1 is defined in (22). Note that $\sigma(2\lambda^2 + \lambda(3\sigma - 2) + \sigma) \geq 0$, so $v_1 \geq 0$. Thus, the largest eigenvalue is negative (and so the origin is stable) if and only if the eigenvalue with the “−” sign before the square root is negative, yielding the condition $\mu > \mu_1^*$, which completes the proof. ■

Remark 3. Note that if $u_s = 0$, then $\mu_1^* = 2\lambda$. This implies that if there is zero effort put in routine screening as a control measure, then condom (social) marketing campaigns have no effect on the epidemic threshold.

The result in Theorem 1 extends our preliminary findings in Frieswijk et al.,³⁸ in which conditions for the (local) stability of the disease-free equilibrium of the behavioral SIS model with a 1-stage negotiation process were established for the limit cases $u_s \ll c - u_m$ and $u_s \gg c - u_m$. These two limit cases can capture extreme scenarios in which the effect of routine screening at STI clinics is negligible with respect to the cost of using protection, or vice versa. On the contrary, Theorem 1 establishes a general result, which characterizes the nontrivial conditions for stability of the disease-free equilibrium over the entire parameter space, and thus allows us to shed light on the role played by the control measures (u_m and u_s), as illustrated in Figure 5 and discussed at the end of the following section.

4.2 | The 2-stage negotiation process

We now consider the 2-stage negotiation process, and we derive the epidemic threshold for the behavioral SIS model. Similar to the 1-stage model, we can derive the set of equations that govern the mean-field evolution of the system from Proposition 2 and the mean-field expressions of (12)–(15), obtaining the following result, whose proof is reported in Appendix C.

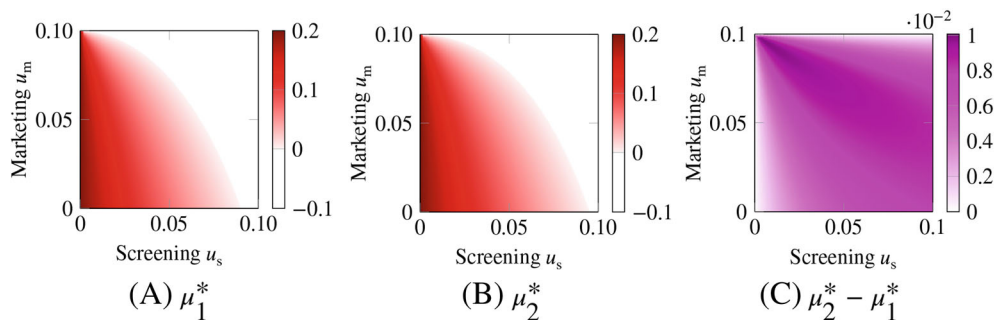


FIGURE 5 Value of the epidemic thresholds computed analytically for different values of the two control parameters modeling the impact of condom marketing (u_m) and routine screening (u_s) for the two different negotiation processes and their comparison. In (A), we show the threshold for the 1-stage negotiation process, μ_1^* ; in (B), the one for the 2-stage negotiation process, μ_2^* . Panel (C) illustrates the difference $\mu_2^* - \mu_1^*$. Common parameters are $\lambda = 0.1$, $\sigma = 0.4$, and $c = 0.1$

Proposition 4. Under Assumption 1 and with the 2-stage negotiation process, the mean-field evolution of the behavioral SIS model is governed by

$$\begin{aligned}
 \dot{s}_{r,j} &= - \left(\bar{\gamma}_{p,j} + u_s + \zeta \frac{1}{n} \sum_{k \in \mathcal{V}} i_{t,k} + \frac{\lambda}{n-1} \sum_{k \in \mathcal{V} \setminus \{j\}} (2i_{r,k} + \sigma(2-\sigma)i_{p,k}) \right) s_{r,j} + \left(\bar{\gamma}_{r,j} + c - u_m - \frac{\lambda\sigma(2-\sigma)}{n-1} \sum_{k \in \mathcal{V} \setminus \{j\}} i_{r,k} \right) s_{p,j}, \\
 \dot{s}_{p,j} &= \left(\bar{\gamma}_{p,j} + u_s + \zeta \frac{1}{n} \sum_{k \in \mathcal{V}} i_{t,k} \right) s_{r,j} - (\bar{\gamma}_{r,j} + c - u_m) s_{p,j} + \beta i_{t,j}, \\
 \dot{i}_{r,j} &= \left(\frac{\lambda}{n-1} \sum_{k \in \mathcal{V} \setminus \{j\}} (2i_{r,k} + \sigma(2-\sigma)i_{p,k}) \right) s_{r,j} + \left(\frac{\lambda\sigma(2-\sigma)}{n-1} \sum_{k \in \mathcal{V} \setminus \{j\}} i_{r,k} \right) s_{p,j} - \left(\bar{\gamma}_{p,j} + \zeta \frac{1}{n} \sum_{k \in \mathcal{V}} i_{t,k} + \mu + u_s \right) i_{r,j} \\
 &\quad + (\bar{\gamma}_{r,j} + c - u_m) i_{p,j}, \\
 \dot{i}_{p,j} &= \left(\bar{\gamma}_{p,j} + \zeta \frac{1}{n} \sum_{k \in \mathcal{V}} i_{t,k} \right) i_{r,j} - (\bar{\gamma}_{r,j} + c - u_m + \mu + u_s) i_{p,j}, \\
 \dot{i}_{t,j} &= (\mu + u_s) i_{r,j} + (\mu + u_s) i_{p,j} - \beta i_{t,j},
 \end{aligned} \tag{27}$$

for all $j \in \mathcal{V}$, where we use the notation

$$\bar{\gamma}_{r,j} := \frac{\sigma(2-\sigma)}{n-1} \sum_{k \in \mathcal{V} \setminus \{j\}} (s_{r,k} + i_{r,k}), \quad \text{and} \quad \bar{\gamma}_{p,j} := \frac{\sigma(2-\sigma)}{n-1} \sum_{k \in \mathcal{V} \setminus \{j\}} (s_{p,k} + i_{p,k}). \tag{28}$$

Observe by comparing Proposition 3 and 4 that the addition of a counter-proposal mechanism to the negotiation process leads to the replacement of σ with $\sigma(2-\sigma)$ in (19) and (20).

The following theorem presents conditions required for (local) asymptotic stability of the disease-free equilibrium for system (27), for a 2-stage negotiation process.

Theorem 2. Consider the behavioral SIS model for a 2-stage negotiation process under Assumption 1, given by (27), in the limit $n \rightarrow \infty$. Then, the system has a unique disease-free equilibrium (with $y_{i,r} = y_{i,p} = y_{i,t} = 0$) which is locally asymptotically stable if and only if

$$\mu > \mu_2^* := -\frac{1}{2}\sigma(2-\sigma) - \frac{1}{2(u_s + c - u_m)} \left[2u_s^2 + (c - u_m)^2 + (c - u_m)(3u_s - 2\lambda) - \lambda\sigma(2-\sigma)u_s - \sqrt{v_2} \right], \tag{29}$$

where

$$\begin{aligned}
 v_2 &:= (c - u_m)^4 + 2(c - u_m)^3 [2\lambda + \sigma(2-\sigma) + u_s] + (c - u_m)^2 [\sigma^2(2-\sigma)^2 + (2\lambda + u_s)^2 + 2\sigma(2-\sigma)(2\lambda + u_s(\lambda + 2))] \\
 &\quad + 2\sigma(2-\sigma)u_s(c - u_m) [2\lambda^2 + \lambda(u_s + 3\sigma(2-\sigma) - 2) + \sigma(2-\sigma) + u_s] + \sigma^2(2-\sigma)^2 u_s^2 (\lambda - 1)^2.
 \end{aligned} \tag{30}$$

Proof. Since Proposition 4 is equivalent to the substitution of σ with $\sigma(2-\sigma)$ in Proposition 3, Theorem 2 is proved by following the proof of Theorem 1 and substituting each occurrence of σ with $\sigma(2-\sigma)$. For the sake of completeness, the complete proof can be found in Appendix D. ■

Observe that $\mu_2^* = 2\lambda$ if there is no effort put toward routine screening as a control action, that is, if $u_s = 0$. Thus, if $u_s = 0$, then there is no effect of condom (social) marketing campaigns on the asymptotic (local) stability of the disease-free equilibrium, and therefore no effect on the eradication of local outbreaks of the disease. This phenomenon is illustrated by the behavior of the epidemic threshold on the left side of Figure 5A,B, for the 1-stage and 2-stage negotiation process, respectively. If some effort is put into routine screening, that is, $u_s > 0$, then the epidemic thresholds μ_1^* and μ_2^* are monotonically decreasing with respect to the control measures u_s and u_m , as shown in Figure 5A,B.

By comparing the two figures, excluding the boundary cases $u_s = 0$ and $u_m = c$, we observe that the inclusion of a counter-proposal mechanism in the negotiation process always leads to an increase in the value of the epidemic threshold, thus making it more difficult to extinguish local outbreaks. This effect is illustrated by Figure 5C, which shows the

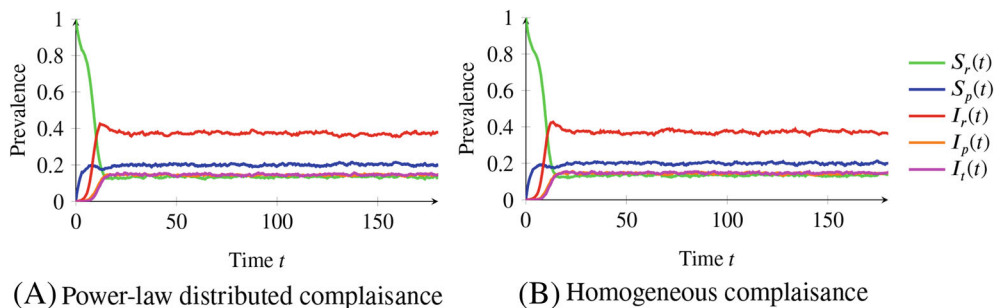


FIGURE 6 Simulations of the behavioral SIS model with (A) heterogeneous and (B) homogeneous levels of complaisance σ for a 1-stage negotiation process. In (A), we distributed complaisance randomly, following a power-law distribution with lower and higher barrier at 0.1 and 1, respectively, and negative exponent equal to -3 , that is, $\mathbb{P}[\sigma_j = \sigma] \propto \sigma^{-3}$. In (B), we set $\sigma_j = 0.4806$, for all $j \in \mathcal{V}$, that is, the average complaisance across the population in (A). Common model parameters are $n = 10\,000$, $\lambda = 0.5$, $u_s = 0.1$, $c = 0.4$, $u_m = 0.1$, $\mu = 0.04$, $\zeta = 1$, and $\beta = 0.5$

difference between the values of μ_2^* and μ_1^* , for different values of the control effort put in the control measures u_s and u_m . For the boundary cases, however, we have a different behavior. In fact, if $u_m = c$, then we have $\mu_1^* = -\sigma - u_s + \lambda\sigma$ and $\mu_2^* = -\sigma(2 - \sigma) - u_s + \lambda\sigma(2 - \sigma)$, which gives $\mu_2^* - \mu_1^* = -\sigma(1 - \sigma)(1 - \lambda) < 0$. If $u_s = 0$, then $\mu_2^* - \mu_1^* = 2\lambda - 2\lambda = 0$.

Hence, we can conclude that, in the presence of routine screening and in the absence of a very strong marketing campaign, the counter-proposal has a negative effect on the stability of the disease-free equilibrium, favoring the inception of epidemic outbreaks and their spread. Therefore, neglecting this behavioral mechanism might lead to a potentially disastrous underestimation of the risk of the spreading of STIs.

Finally, we recall that our theoretical results were derived under the assumption that all the individuals have the same level of complaisance, that is, $\sigma_j = \sigma$, for all $j \in \mathcal{V}$. However, the simulations illustrated in Figure 6 suggest that our theoretical findings obtained under the assumption that the population is homogeneous might still be applied as a good proxy for heterogeneous populations, since heterogeneity in σ seems to have a negligible effect on the spread of the disease. In fact, the temporal evolution of the system with highly heterogeneous complaisance across the population, in Figure 6A, appears not to differ sensibly from the one of a system with homogeneous complaisance equal to the average of the heterogeneous one, in Figure 6B. The results illustrated in Figure 6 are obtained while considering a 1-stage negotiation process. Similar results (here omitted) are obtained for a 2-stage negotiation process. Hence, it seems that the complaisance may be approximated as homogeneous across the population.

5 | SIMULATIONS

In this section, we employ numerical simulations to extend our theoretical findings. The formulation of the model as a Markov process allows us to perform fast Monte Carlo simulations of the dynamics.⁴⁹ Specifically, we investigate the role of the partner network on the spreading of STIs and assess the effectiveness of partner notification as a control measure. In all our simulations we consider the same population of $n = 10\,000$ individuals, and, for each simulation, we generate a partner network in which a fixed fraction of the population (50%, in our simulations) is involved in a dyadic relationship, while the rest of the population is not involved in any relation. These relations are generated uniformly at random, utilizing a method similar to a configuration model.⁵⁰ Observe that, for the sake of simplicity, we neglect polyamorous relations in our simulations.

We investigate the role of the partner network by comparing the outcome of the behavioral SIS model for different values of faithfulness and complaisance. Specifically, we perform Monte Carlo simulations of the system (averaged over 100 independent runs) to estimate the long-run infection prevalence, measured as $I_p(t_{\text{end}}) + I_r(t_{\text{end}}) + I_t(t_{\text{end}})$, where $t_{\text{end}} = 200$ is the time-window of our simulations. For the sake of simplicity, and considering our observations in the previous section based on Figure 6, we assume that all individuals have the same level of complaisance, that is, $\sigma_j = \sigma$, for all $j \in \mathcal{V}$, and that all individuals involved in relationships have the same degree of faithfulness, that is, $p_j = p$, for all $j \in \mathcal{V}$ with $\mathcal{P}_j \neq \emptyset$. Hence, we estimate the epidemic infection prevalence for complaisance levels ranging from 0 to 1—which model the limit cases of a completely stubborn and an easy-to-persuade population, respectively—and

faithfulness levels that range from 0 to 1, representing the extreme cases of an always-cheating and a never-cheating population.

Our findings, illustrated in Figure 7, confirm the intuition that casual partners can play a key role in the spread of STIs, consistent with the findings in Vajdi et al.²⁸ In fact, as the level of faithfulness decreases (i.e., a higher fraction of the individuals have extra-relationship encounters), the long-run epidemic prevalence increases. It is interesting to notice in Figure 7A,B that, for STIs with a small per-contact infection probability ($\lambda = 0.1$), faithfulness can determine whether the system is in a fast-extinction regime (white region) or if the disease becomes endemic (red region, where the intensity is the estimated prevalence at the endemic equilibrium). Predictably, we also observe that the maximum effect of the counter proposal is achieved at intermediate values of σ , that is, for those values in the neighborhood of $\sigma = 0.5$, which maximizes the fraction of counter proposals made and accepted—which is equal to $\sigma(1 - \sigma)$. Furthermore, we observe that the system exhibits a nontrivial interplay between individuals' complaisance, the infection probability, and the nature of the negotiation process on the long-run epidemic prevalence. While the addition of a counter-proposal always favors the spread of the infection, its effect is not uniform. Specifically, we observe that the counter-proposal has an extremely strong impact for small values of the per-contact infection probability, where it may cause the system to switch from the fast-extinction regime to the one where the infection becomes endemic, while the impact becomes milder for extremely contagious diseases (compare Figure 7C with F).

Finally, we investigate the effectiveness of partner notification as a control measure. To this aim, we consider two different scenarios—in the presence of the other control measures u_s and u_m , and in their absence—and we assess the impact of increasing the enforcement level of partner notification u_n up to 2, for different levels of faithfulness p . In order to visualize such an impact, we report the difference in the long-run epidemic prevalence with respect to the scenario with no partner notification ($u_n = 0$). Our findings, summarized in Figure 8, suggest that partner notification is a very effective control measure, in particular when combined with other control measures (Figure 8B). When no other measures are implemented, its impact is still non-negligible, especially for faithful populations (see Figure 8A for p large). Clearly, in the limit case $p = 1$, individuals involved in a romantic partnership have no casual encounters, limiting the need and impact of notifications. The decreasing effectiveness for unfaithful population suggests that extending such a notification measure to trace casual contacts might be a valuable technique to further combat the spread of STIs.

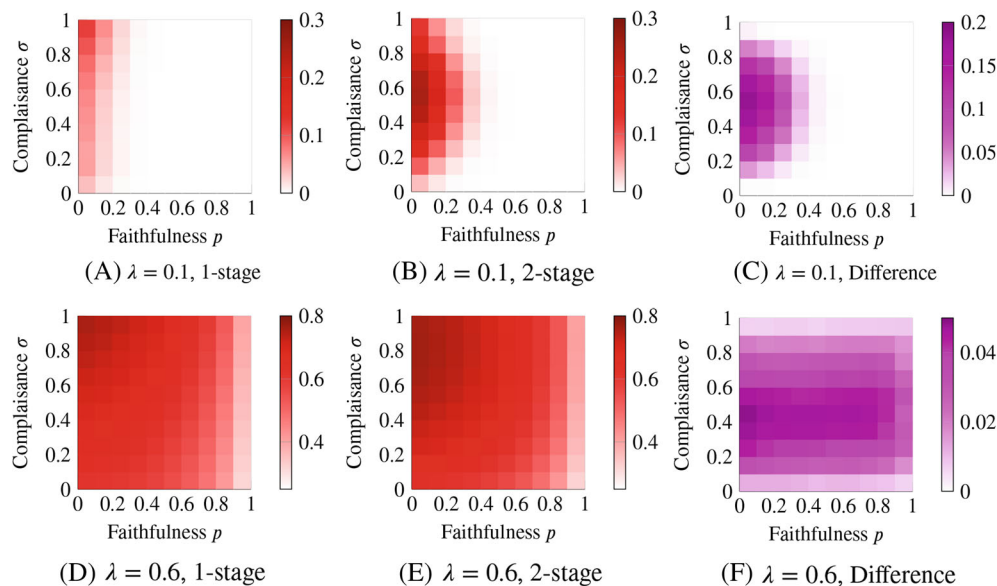


FIGURE 7 Monte Carlo estimation (over 100 independent runs) of the long-run epidemic prevalence $I_p + I_r + I_s$, measured at time $t_{\text{end}} = 200$ (intensity of red) for different values of faithfulness p and complaisance σ , for (A–C) $\lambda = 0.1$ and (D–F) $\lambda = 0.6$, for the 1-stage (in (A,D)) and the 2-stage (in (B,E)) negotiation process. Panels (C,F) show the difference in the long-run prevalence between the two negotiation processes (intensity of violet). Common parameters are: $n = 10\,000$, $\mu = 0.04$, $c = 0.5$, $\zeta = 1$, $\beta = 0.5$, $u_s = 0.1$, $u_m = 0.1$, and $u_n = 0$. The partner network is generated at random, with 50% of the individuals involved in a dyadic relation, and the rest not involved in any relation

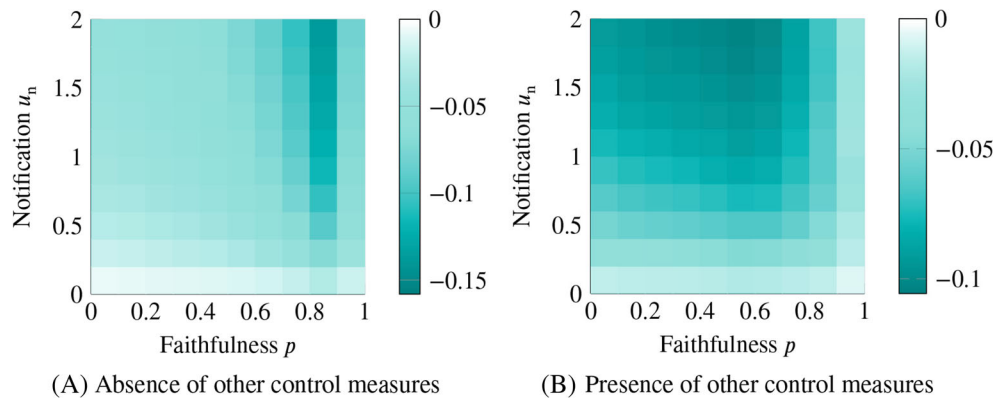


FIGURE 8 Monte Carlo estimation (over 100 independent runs) of the decrease in the long-run epidemic prevalence $I_p + I_r + I_t$ (measured at time $t_{\text{end}} = 200$) as an effect of partner notification u_n (intensity of cyan) for different values of faithfulness p , in the absence of control measures u_s and u_m (in (A)) and in their presence (in (B)). Common parameters are: $n = 10\,000$, $\mu = 0.04$, $c = 0.5$, $\zeta = 1$, $\beta = 0.5$, $\lambda = 0.5$, and $\sigma = 0.4$, where we consider a 1-stage negotiation process. In (B), $u_s = u_m = 0.1$. The partner network is generated at random, with 50% of the individuals involved in a dyadic relation, and the rest not involved in any relation

6 | CONCLUSION

We proposed a time-varying network model for the spread of STIs, which accounts for behavioral preferences, and considers two distinct negotiation processes between nonpartners on the use of protective measures. Our epidemic model allows to cast light on the role of condom (social) marketing campaigns, routine screening at STI clinics, and partner notification in the spreading of STIs. Employing a mean-field approach in the limit or large-scale populations, we analytically derived the epidemic threshold for both negotiation processes, in the absence of a partner backbone. Our theoretical results indicate that routine screening is crucial in the eradication of local outbreaks, whereas marketing campaigns are beneficial only if combined with routine screening. The formulation of the model as a Markov process enables its further analysis via fast Monte Carlo numerical simulations.⁴⁹ Thus, we numerically examined the role of partner networks in the spreading, for different levels of complaisance and faithfulness. The simulations illustrate the negative impact of the addition of a counter-proposal in the negotiation process on the spread of the infection, which especially forms a problem for small values of the per-contact infection probability. Furthermore, simulations showed that partner notification is mainly effective when combined with screening and marketing campaigns, but still has some impact as a sole measure for populations with a high degree of faithfulness.

The model proposed in this article and its analysis rely on some simplifying assumptions. However, due to its flexibility, many additional features can be incorporated in the modeling framework without fundamentally changing its fabric. First, we have assumed that all the individuals have the same tendency to initiate sexual encounters. Moreover, sexual encounters are generated without considering gender and sexual orientation of individuals. However, heterogeneity and further constraints can be straightforwardly incorporated in the formation process of the network of sexual initiatives, similar to continuous-time ADNs.^{32,38,42}

For future research, one could incorporate these features within the modeling framework and thereby extend both the theoretical and the numerical analysis of the model. These extensions would also allow to consider other aspects of sexual behavior, as well as asymmetries and heterogeneity in the per-encounter infection probabilities depending on individuals' gender and sexual orientation.⁵¹ Besides these generalizations, an analytical treatment of the dynamical system above the epidemic threshold is still missing, and it will be an important direction for future theoretical studies. Our model incorporates several control actions, captured by different control parameters. However, a rigorous technique to map the implementation of real-world control actions into changes in the model parameters is still an open problem, calling for the use of real-world data to calibrate the model. In particular, one may use data from existing surveys and design questionnaires to calibrate these parameters. For instance, the question “Did you start/stop using condoms? If so, for which main reason?” can be used to determine the relative magnitude of the model parameters involved in the corresponding behavioral transitions, while changes in the outcome of these surveys from before to after a marketing campaign can be used to estimate its impact. Furthermore, in view of the good effectiveness of partner

notification registered in our simulations, future research may consider extending such a control measure to include tracing of casual encounters happened during a restrictive time period before diagnosis.³⁴ Finally, a better understanding of the very nature of real-life negotiation processes should be achieved. Experimental sociological studies might be designed and performed to this aim. The inclusion of these further features and the design of experimentally-grounded negotiation processes will finally allow us to validate the proposed model against real-world data on the spread of STIs.

ACKNOWLEDGMENTS

The work was partially supported by the European Research Council (ERC-CoG-771687).

CONFLICT OF INTEREST

The authors declare no potential conflict of interests.

DATA AVAILABILITY STATEMENT

The code used to produce the results of this manuscript is available at <https://github.com/lzino90/sti>. The data that support the findings of this study are available from the corresponding author upon reasonable request.

ORCID

Kathinka Frieswijk  <https://orcid.org/0000-0003-3386-4908>

Lorenzo Zino  <https://orcid.org/0000-0002-0946-6523>

Ming Cao  <https://orcid.org/0000-0001-5472-562X>

REFERENCES

- Gross G, Tyring SK. *Sexually Transmitted Infections and Sexually Transmitted Diseases*. 1st ed. Springer; 2011.
- Centers for Disease Control and Prevention. CDC estimates 1 in 5 people in the U.S. have a sexually transmitted infection. Accessed September 2021. <https://www.cdc.gov/media/releases/2021/p0125-sexually-transmitted-infection.html>.
- Rowley J, Vander Hoorn S, Korenromp E, et al. Chlamydia, gonorrhoea, trichomoniasis and syphilis: global prevalence and incidence estimates, 2016. *Bull World Health Organ*. 2019;97(8):548-562. doi:10.2471/BLT.18.228486
- Martin MJ, Thottathil SE, Newman TB. Antibiotics overuse in animal agriculture: a call to action for health care providers. *Am J Public Health*. 2015;105(12):2409-2410. doi:10.2105/AJPH.2015.302870
- Pechère JC. Patients' interviews and misuse of antibiotics. *Clin Infect Dis*. 2001;33(Supplement 3):S170-S173. doi:10.1086/321844
- Wi T, Lahra MM, Ndowa F, et al. Antimicrobial resistance in *Neisseria gonorrhoeae*: global surveillance and a call for international collaborative action. *PLoS Med*. 2017;14(7):e1002344. doi:10.1371/journal.pmed.1002344
- Centers for Disease Control and Prevention. Sexually Transmitted Disease Surveillance 2019. Accessed September 2021. <https://www.cdc.gov/std/statistics/2019/default.htm>.
- World Health Organization. Disruption in HIV, Hepatitis and STI services due to COVID-19. Accessed September 2021. <https://www.who.int/hiv/data/en>.
- Tao J, Napoleon SC, Maynard MA, et al. Impact of the COVID-19 pandemic on sexually transmitted infection clinic visits. *Sex Transm Dis*. 2021;48(1):e5-e7. doi:10.1097/OLQ.0000000000001306
- Cusini M, Benardon S, Vidoni G, Brignolo L, Veraldi S, Mandolini PL. Trend of main STIs during COVID-19 pandemic in Milan. *Italy Sex Transm Infect*. 2021;97(2):99-99. doi:10.1136/sextrans-2020-054608
- Farley TA, Cohen DA, Elkins W. Asymptomatic sexually transmitted diseases: the case for screening. *Prev Med*. 2003;36(4):502-509. doi:10.1016/s0091-7435(02)00058-0
- Holmes K, Levine R, Weaver M. Effectiveness of condoms in preventing sexually transmitted infections. *Bull World Health Organ*. 2004;82(6):454-461. doi:10.1590/S0042-96862004000600012
- Pastor-Satorras R, Castellano C, Van Mieghem P, Vespignani A. Epidemic processes in complex networks. *Rev Mod Phys*. 2015;87(3):925-979. doi:10.1103/RevModPhys.87.925
- Nowzari C, Preciado VM, Pappas GJ. Analysis and control of epidemics: a survey of spreading processes on complex networks. *IEEE Control Syst Mag*. 2016;36(1):26-46. doi:10.1109/MCS.2015.2495000
- Mei W, Mohagheghi S, Zampieri S, Bullo F. On the dynamics of deterministic epidemic propagation over networks. *Annu Rev Control*. 2017;44:116-128. doi:10.1016/j.arcontrol.2017.09.002
- Paré PE, Beck CL, Başar T. Modeling, estimation, and analysis of epidemics over networks: an overview. *Annu Rev Control*. 2020;50:345-360. doi:10.1016/j.arcontrol.2020.09.003
- Zino L, Cao M. Analysis, prediction, and control of epidemics: a survey from scalar to dynamic network models. *IEEE Circuits Syst Mag*. 2021;21(4):4-23. doi:10.1109/MCAS.2021.3118100
- Holme P. Modern temporal network theory: a colloquium. *The European Phys J B*. 2015;88(9):234. doi:10.1140/epjb/e2015-60657-4

19. Paré PE, Beck CL, Nedić A. Epidemic processes over time-varying networks. *IEEE Trans Control Network Syst.* 2018;5(3):1322-1334. doi:10.1109/TCNS.2017.2706138
20. Brauer F, Castillo-Chavez C. *Mathematical Models in Population Biology and Epidemiology*. 1st ed. Springer; 2012.
21. Giordano G, Blanchini F, Bruno R, et al. Modelling the COVID-19 epidemic and implementation of population-wide interventions in Italy. *Nat Med.* 2020;26:855-860. doi:10.1038/s41591-020-0883-7
22. Della Rossa F, Salzano D, Di Meglio A, et al. A network model of Italy shows that intermittent regional strategies can alleviate the COVID-19 epidemic. *Nat Commun.* 2020;11(1):5106. doi:10.1038/s41467-020-18827-5
23. Brauner JM, Mindermann S, Sharma M, et al. Inferring the effectiveness of government interventions against COVID-19. *Science.* 2021;371(6531):eabd9338. doi:10.1126/science.abd9338
24. Funk S, Gilad E, Watkins C, Jansen VAA. The spread of awareness and its impact on epidemic outbreaks. *Proc Natl Acad Sci U S A.* 2009;106(16):6872-6877. doi:10.1073/pnas.0810762106
25. Sahneh FD, Chowdhury FN, Scoglio CM. On the existence of a threshold for preventive behavioral responses to suppress epidemic spreading. *Sci Rep.* 2012;2(1):632. doi:10.1038/srep00632
26. Granell C, Gomez S, Arenas A. Dynamical interplay between awareness and epidemic spreading in multiplex networks. *Phys Rev Lett.* 2013;111(12):128701. doi:10.1103/PhysRevLett.111.128701
27. Eames K, Keeling M. Modeling dynamic and network heterogeneities in the spread of sexually transmitted diseases. *Proc Natl Acad Sci U S A.* 2002;99(20):13330-13335. doi:10.1073/pnas.202244299
28. Vajdi A, Juher D, Saldaña J, Scoglio C. A multilayer temporal network model for STD spreading accounting for permanent and casual partners. *Sci Rep.* 2020;10(1):1-12. doi:10.1038/s41598-020-60790-0
29. Yan S, Zhang Y, Ma J, Yuan S. An edge-based SIR model for sexually transmitted diseases on the contact network. *J Theor Biol.* 2018;439:216-225. doi:10.1016/j.jtbi.2017.12.003
30. Hethcote HW, Yorke JA. *Gonorrhoea Transmission Dynamics and Control*. 1st ed. Springer; 1984.
31. Perra N, Gonçalves B, Pastor-Satorras R, Vespignani A. Activity driven modeling of time varying networks. *Sci Rep.* 2012;2:469. doi:10.1038/srep00469
32. Zino L, Rizzo A, Porfiri M. Continuous-time discrete-distribution theory for activity-driven networks. *Phys Rev Lett.* 2016;117(22). doi:10.1103/PhysRevLett.117.228302
33. Sweat MD, Denison J, Kennedy C, Tedrow V, O'Reilly K. Effects of condom social marketing on condom use in developing countries: a systematic review and meta-analysis, 1990–2010. *Bull World Health Organ.* 2012;90(8):557-632. doi:10.2471/BLT.11.094268
34. Althaus CL, Turner KM, Mercer CH, et al. Effectiveness and cost-effectiveness of traditional and new partner notification technologies for curable sexually transmitted infections: observational study, systematic reviews and mathematical modelling. *Health Technol Assess.* 2014;18(2):1-100. doi:10.3310/hta18020
35. Bell G, Ward H, Day S, et al. Partner notification for gonorrhoea: a comparative study with a provincial and a metropolitan UK clinic. *Sex Transm Infect.* 1998;74(6):409-414. doi:10.1136/sti.74.6.409
36. Gorbach PM, Aral SO, Celum C, et al. To notify or not to notify: STD patients' perspectives of partner notification in Seattle. *Sex Transm Dis.* 2000;27(4):193-200. doi:10.1097/00007435-200004000-00003
37. Van Mieghem P, Omic J, Kooij R. Virus spread in networks. *IEEE/ACM Trans Networking.* 2009;17(1):1-14. doi:10.1109/TNET.2008.925623
38. Frieswijk K, Zino L, Cao M. Modelling behavioural preferences in epidemic models for sexually transmitted infections on temporal networks. Proceedings of the 2021 European Control Conference (ECC) 2021. https://research.rug.nl/files/171628409/ECC21_0118_FI.pdf
39. Bailey NTJ. *The Elements of Stochastic Processes with Applications to the Natural Sciences*. 1st ed. John Wiley & Sons; 1990.
40. Levin DA, Peres Y, Wilmer EL. *Markov Chains and Mixing Times*. 1st ed. American Mathematical Society; 2006.
41. Levine EC, Herbenick D, Martinez O, Fu TC, Dodge B. Open relationships, nonconsensual nonmonogamy, and monogamy among U.S. adults: findings from the 2012 national survey of sexual health and behavior. *Arch Sex Behav.* 2018;47(5):1439-1450. doi:10.1007/s10508-018-1178-7
42. Zino L, Rizzo A, Porfiri M. An analytical framework for the study of epidemic models on activity driven networks. *J Complex Networks.* 2017;5(6):924-952. doi:10.1093/comnet/cnx056
43. Samuelson W, Zeckhauser R. Status quo bias in decision making. *J Risk Uncertainty.* 1988;1:7-59. doi:10.1007/BF00055564
44. Alós-Ferrer C, Hügelschäfer S, Li J. Inertia and decision making. *Front Psychol.* 2016;7:169. doi:10.3389/fpsyg.2016.00169
45. Sarkar DNN. Barriers to condom use. *Eur J Contracept Reprod Health Care.* 2008;13(2):114-122. doi:10.1080/13625180802011302
46. Ye M, Zino L, Rizzo A, Cao M. Game-theoretic modeling of collective decision making during epidemics. *Phys Rev E.* 2021;104:024314. doi:10.1103/PhysRevE.104.024314
47. Zino L, Rizzo A, Porfiri M. On assessing control actions for epidemic models on temporal networks. *IEEE Control Syst Lett.* 2020;4(4):797-802. doi:10.1109/LCSYS.2020.2993104
48. Kurtz TG. Limit theorems for sequences of jump Markov processes approximating ordinary differential processes. *J Appl Prob.* 1971;8(2):344-356. doi:10.2307/3211904
49. Gillespie TD. A general method for numerically simulating the stochastic time evolution of coupled chemical reactions. *J Comput Phys.* 1976;22(4):403-434. doi:10.1016/0021-9991(76)90041-3
50. Newman M. *Networks: An Introduction*. 1st ed. Oxford University Press; 2010.
51. Lewis J, White PJ, Price MJ. Per-partnership transmission probabilities for chlamydia trachomatis infection: evidence synthesis of population-based survey data. *Int J Epidemiol.* 2020;50(2):510-517. doi:10.1093/ije/dyaa202

How to cite this article: Frieswijk K, Zino L, Cao M. A time-varying network model for sexually transmitted infections accounting for behavior and control actions. *Int J Robust Nonlinear Control*. 2023;33(9):4784-4807. doi: 10.1002/rnc.5930

APPENDIX A. MEAN-FIELD EXPRESSIONS OF THE TRANSITION RATES

The mean-field expressions of the transition rates in matrix Q_j in (6) can be obtained by substituting the indicator functions in the sums in $\kappa_{r,j}$, $\kappa_{p,j}$, $v_{r,j}$, and $v_{p,j}$ with the corresponding probabilities defined in (16). For the 1-stage negotiation process and $j \in \mathcal{V}$, we obtain from (8)–(11):

$$\begin{aligned} \tilde{\kappa}_{r,j} = \tilde{\kappa}_{r,j}^{(1)} = & \lambda \left(\frac{p_j}{|\mathcal{P}_j|} \sum_{k \in \mathcal{P}_j} (i_{r,k} + i_{p,k}) + \frac{1-p_j}{n-1-|\mathcal{P}_j|} \left[\sum_{k \in \mathcal{V} \setminus \{\mathcal{P}_j\}} (1-p_k) i_{r,k} + \sum_{k \in \mathcal{V} \setminus \{\mathcal{P}_j\}} (1-p_k) \sigma_k i_{p,k} \right] \right) \\ & + \lambda \left(\sum_{k \in \mathcal{P}_j} \frac{p_k}{|\mathcal{P}_k|} i_{r,k} + (1-p_j) \sum_{k \in \mathcal{V} \setminus \{\mathcal{P}_j\}} \frac{1-p_k}{n-1-|\mathcal{P}_k|} i_{r,k} \right), \end{aligned} \quad (\text{A1})$$

$$\tilde{\kappa}_{p,j} = \tilde{\kappa}_{p,j}^{(1)} = \lambda \left(\sum_{k \in \mathcal{P}_j} \frac{p_k}{|\mathcal{P}_k|} i_{r,k} + (1-p_j) \sigma_j \sum_{k \in \mathcal{V} \setminus \{\mathcal{P}_j\}} \frac{1-p_k}{n-1-|\mathcal{P}_k|} i_{r,k} \right), \quad (\text{A2})$$

$$\tilde{v}_{r,j} = \tilde{v}_{r,j}^{(1)} = \sum_{k \in \mathcal{P}_j} \frac{p_k}{|\mathcal{P}_k|} (s_{r,k} + i_{r,k}) + (1-p_j) \sigma_j \sum_{k \in \mathcal{V} \setminus \{\mathcal{P}_j\}} \frac{1-p_k}{n-1-|\mathcal{P}_k|} (s_{r,k} + i_{r,k}), \quad (\text{A3})$$

$$\tilde{v}_{p,j} = \tilde{v}_{p,j}^{(1)} = \sum_{k \in \mathcal{P}_j} \frac{p_k}{|\mathcal{P}_k|} (s_{p,k} + i_{p,k}) + (1-p_j) \sigma_j \sum_{k \in \mathcal{V} \setminus \{\mathcal{P}_j\}} \frac{1-p_k}{n-1-|\mathcal{P}_k|} (s_{p,k} + i_{p,k}). \quad (\text{A4})$$

For the 2-stage negotiation process, (12)–(15) yield

$$\tilde{\kappa}_{r,j} = \tilde{\kappa}_{r,j}^{(2)} = \tilde{\kappa}_{r,j}^{(1)} + \lambda(1-p_j)(1-\sigma_j) \sum_{k \in \mathcal{V} \setminus \{\mathcal{P}_j\}} \frac{\sigma_k(1-p_k)}{n-1-|\mathcal{P}_k|} i_{p,k}, \quad (\text{A5})$$

$$\tilde{\kappa}_{p,j} = \tilde{\kappa}_{p,j}^{(2)} = \tilde{\kappa}_{p,j}^{(1)} + \lambda \sigma_j \frac{1-p_j}{n-1-|\mathcal{P}_j|} \sum_{k \in \mathcal{V} \setminus \{\mathcal{P}_j\}} (1-p_k)(1-\sigma_k) i_{r,k}, \quad (\text{A6})$$

$$\tilde{v}_{r,j} = \tilde{v}_{r,j}^{(2)} = \tilde{v}_{r,j}^{(1)} + \sigma_j \frac{1-p_j}{n-1-|\mathcal{P}_j|} \sum_{k \in \mathcal{V} \setminus \{\mathcal{P}_j\}} (1-p_k)(1-\sigma_k) (s_{r,k} + i_{r,k}), \quad (\text{A7})$$

$$\tilde{v}_{p,j} = \tilde{v}_{p,j}^{(2)} = \tilde{v}_{p,j}^{(1)} + \sigma_j \frac{1-p_j}{n-1-|\mathcal{P}_j|} \sum_{k \in \mathcal{V} \setminus \{\mathcal{P}_j\}} (1-p_k)(1-\sigma_k) (s_{p,k} + i_{p,k}). \quad (\text{A8})$$

APPENDIX B. PROOF OF PROPOSITION 3

Proof. Let us consider the 1-stage negotiation process. Note that under Assumption 1, the rate of the Poisson clock associated with the contagion process of individual $j \in \mathcal{V}$ in (A1) reduces to

$$\tilde{\kappa}_{r,j}^{(1)} = \frac{\lambda}{n-1} \left(\sum_{k \in \mathcal{V} \setminus \{j\}} 2i_{r,k} + \sum_{k \in \mathcal{V} \setminus \{j\}} \sigma_k i_{p,k} \right) = \frac{\lambda}{n-1} \sum_{k \in \mathcal{V} \setminus \{j\}} (2i_{r,k} + \sigma_k i_{p,k}), \quad (\text{B1})$$

as the first and fourth terms in (A1) are omitted, while the others can be simplified (since $\mathcal{P}_j = \emptyset$, $p_j = 0$, and $\sigma_j = \sigma$, for all $j \in \mathcal{V}$). Likewise, for (A2)–(A4), we respectively find the following mean-field expressions, under Assumption 1:

$$\tilde{\kappa}_{p,j}^{(1)} = \frac{\lambda\sigma}{n-1} \sum_{k \in \mathcal{V} \setminus \{j\}} i_{r,k}, \quad \tilde{v}_{r,j}^{(1)} = \frac{\sigma}{n-1} \sum_{k \in \mathcal{V} \setminus \{j\}} (s_{r,k} + i_{r,k}) = \gamma_{r,j}, \quad \tilde{v}_{p,j}^{(1)} = \frac{\sigma}{n-1} \sum_{k \in \mathcal{V} \setminus \{j\}} (s_{p,k} + i_{p,k}) = \gamma_{p,j}, \quad (B2)$$

as defined in (20). Finally, plugging this in (17) immediately yields (19), where $\eta_j = 0$ because of Assumption 1. ■

APPENDIX C. PROOF OF PROPOSITION 4

Proof. Let us consider the 2-stage negotiation process. Under Assumption 1, (A5) simplifies to

$$\tilde{\kappa}_{r,j}^{(2)} = \frac{\lambda}{n-1} \left(\sum_{k \in \mathcal{V} \setminus \{j\}} 2i_{r,k} + \sum_{k \in \mathcal{V} \setminus \{j\}} \sigma(2-\sigma)i_{p,k} \right) = \frac{\lambda}{n-1} \sum_{k \in \mathcal{V} \setminus \{j\}} (2i_{r,k} + \sigma(2-\sigma)i_{p,k}). \quad (C1)$$

Similarly, rates in (A6)–(A8) respectively yield the following mean-field expressions:

$$\tilde{\kappa}_{p,j}^{(2)} = \frac{\lambda\sigma(2-\sigma)}{n-1} \sum_{k \in \mathcal{V} \setminus \{j\}} i_{r,k}, \quad \tilde{v}_{r,j}^{(2)} = \frac{\sigma(2-\sigma)}{n-1} \sum_{k \in \mathcal{V} \setminus \{j\}} (s_{r,k} + i_{r,k}) = \bar{\gamma}_{r,j}, \quad \tilde{v}_{p,j}^{(2)} = \frac{\sigma(2-\sigma)}{n-1} \sum_{k \in \mathcal{V} \setminus \{j\}} (s_{p,k} + i_{p,k}) = \bar{\gamma}_{p,j}, \quad (C2)$$

as in (28). Plugging this in (17), while noting that $\eta_j = 0$ for all $j \in \mathcal{V}$ due to Assumption 1, we obtain (27). ■

APPENDIX D. PROOF OF THEOREM 2

Proof. The proof has a similar structure to the one of Theorem 1, so we report just the main computations. First, we observe that the disease-free equilibrium of (27) is unique and coincides with (23). Then, by considering the system of four independent macroscopic variables, performing the same change of variables in (24), and linearising about the origin (i.e., the disease-free equilibrium), we obtain the following system of equations:

$$\begin{aligned} \dot{y}_q &= -(u_s + c - u_m)y_q - \left(\sigma(2-\sigma)\frac{u_s}{u_s + c - u_m} + u_s \right) y_{i,r} + \left(\sigma(2-\sigma) \left(1 - \frac{u_s}{u_s + c - u_m} \right) - u_s \right) y_{i,p} \\ &\quad + \left(\zeta \left(1 - \frac{u_s}{u_s + c - u_m} \right) + \beta - u_s \right) y_{i,t}, \\ \dot{y}_{i,r} &= \left([\sigma(2-\sigma)(\lambda-1) - 2\lambda] \frac{u_s}{u_s + c - u_m} + 2\lambda - u_s - \mu \right) y_{i,r} + \left(\sigma(2-\sigma)(\lambda+1) \left(1 - \frac{u_s}{u_s + c - u_m} \right) + c - u_m \right) y_{i,p}, \\ \dot{y}_{i,p} &= \sigma(2-\sigma)\frac{u_s}{u_s + c - u_m} y_{i,r} - \left(\sigma(2-\sigma) \left(1 - \frac{u_s}{u_s + c - u_m} \right) + c - u_m + \mu + u_s \right) y_{i,p}, \\ \dot{y}_{i,t} &= (\mu + u_s)y_{i,r} + (\mu + u_s)y_{i,p} - \beta y_{i,t}. \end{aligned} \quad (D1)$$

We compute the eigenvalues of the Jacobian matrix, obtaining two that are always negative, namely, $-(u_s + c - u_m) < 0$ and $-\beta < 0$, and

$$-\mu - \frac{1}{2}\sigma(2-\sigma) - \frac{1}{2(u_s + c - u_m)} \left[2u_s^2 + (c - u_m)^2 + (c - u_m)(3u_s - 2\lambda) - \lambda\sigma(2-\sigma)u_s \pm \sqrt{v_2} \right], \quad (D2)$$

where v_2 is defined in (30). Finally, we observe that $\sigma(2-\sigma)[2\lambda^2 + \lambda(3\sigma(2-\sigma) - 2) + \sigma(2-\sigma)] \geq 0$, so $v_2 \geq 0$. Hence, we conclude that the largest eigenvalue is negative if and only if $\mu > \mu_2^*$. ■